Transport properties and Stokes-Einstein relation in a computer-simulated glass-forming Cu_{33.3}Zr_{66.7} melt

X. J. Han and H. R. Schober

Phys. Rev. B **83**, 224201 — Published 17 June 2011

DOI: 10.1103/PhysRevB.83.224201

Transport properties and Stokes-Einstein relation in computer simulated glass forming $Cu_{33.3}Zr_{66.7}$ melt

X. J. Han[1, 2,*] and H. R. Schober[2,†]

1. School of Materials Science and Engineering, Shanghai Jiao Tong University, Dongchuan Rd. 800, 200240 Shanghai, P. R. China

2. Institut für Festkörperforschung, Forschungszentrum Jülich, 52425 Jülich, Germany

Abstract

Molecular dynamics simulation with a modified embedded atom potential was used to study transport properties and the Stokes-Einstein relation of a glass-forming $Cu_{33.3}Zr_{66.7}$ metallic melt. Upon cooling, at high temperatures, the self-diffusion coefficients of the two species evolve nearly parallel, whereas they diverge below 1600K. The viscosity as function of temperature is calculated from the Green-Kubo equation. The critical temperature of mode coupling theory, T_c, is found as 1030K, both, from the transport properties and the α-relaxation time. It is found that the Stokes-Einstein relation between viscosity and diffusivity breaks down at around 1600K, far above T_c and even above the melting temperature. The temperature dependence of the effective diameter in the Stokes-Einstein relation correlates closely with the first derivative of the ratio of the self-diffusion coefficients of the two components. We propose that the onset of Stokes-Einstein relation breakdown could be predicted quantitatively by the divergence behavior of diffusion coefficients, and the breakdown of Stokes-Einstein relation is ascribed to the sudden increase of the dynamics heterogeneity.

PACS number(s): 66.20.Cy, 66.10.cg, 02.70.Ns

I. INTRODUCTION

Transport properties, such as the shear viscosity and the diffusion coefficients, of liquid metals, especially in the metastable undercooled regime, are kinetic key parameters that determine the crystal nucleation and growth in metallic melts. They also play a very important role in studying the liquid-to-glass transition in a glass forming system, which is still an open question up to now. According to the free volume theory, [1] the free volume of liquids can be derived from the transport properties of the liquid. The free volume of liquids correlates with that of glassy alloys, which determines the strength and ductility of metallic glasses. [2] Thus, transport properties of liquids could reveal valuable information about mechanical properties of metallic glasses and, therefore, have attracted extensive research interest. [3-7]

In simple liquids, the self-diffusion coefficient is often related to the shear viscosity by the Stokes-Einstein (SE) relation [8, 9]

$$D = \frac{k_B T}{c \pi \eta d}, \tag{1}$$

where k_B is the Boltzmann constant, d the effective diameter of the particle, and c a constant that depends on the boundary conditions. It is 3 for "stick" boundary condition and 2 for "slip" boundary condition.

For some molecular liquids [10] and metallic glass forming systems, [11-13] the SE relation holds quite well at temperatures above the critical temperature T_c of the mode coupling theory (MCT) [14] and breaks down at temperatures below. According to MCT, T_c characterizes a change in the dynamics of the liquid from ergodic liquid-like flow to non-ergodic solid-like hopping. Therefore, a breakdown of the SE relation around T_c seems quite reasonable. However, some experiments indicate that the SE relation may already break down at

temperatures far above T_c.[15-17] Noticeably, Meyer *et al.* found that in a Zr-Ti-Cu-Ni-Be melt the mobility of Ni and Ti atoms remains decoupled from viscous flow far above the mode coupling T_c and the liquidus temperature, T_L.[16] This implies that T_c is not necessarily the temperature that determines the breakdown of the SE relation. The temperature T_s, marking the onset of the breakdown of the SE relation, might be different. Clearly, T_s is determined by the dynamics of the liquid. Its relation to T_L, T_c and T_g, , however, is not clear. Why the SE relation can break down far above the mode coupling T_c and even above the liquidus temperature, and how empirically to predict T_s are still open questions. An investigation of these questions is not only meaningful for the understanding of the change in the dynamics at the liquid-to-glass transition, but also informative for experimentalists since they often approximate the self-diffusion coefficient via the SE relation from the viscosity, or vice versa.

Molecular dynamics simulation allows an insight into the dynamics on an atomic level. The breakdown of the SE relation was addressed by several calculations simulating real and model liquids. A breakdown of the SE relation was observed in systems as diverse as liquids of hard [18] and soft spheres,[19] binary Lennard-Jones fluids,[20, 21] water[22] and silica melts.[23] These simulations have, so far, not lead to a unique, accepted picture.

To elucidate the relation between the viscosity and the self-diffusion coefficients, we must determine both properties accurately. In experiment the determination of transport properties in the metastable undercooled regime is rather challenging, because any contact of the metallic melt with the container wall immediately induces crystallization of the melt.[24] This is the reason why experimental studies of viscosity and self-diffusion coefficients are normally confined to the normal liquid regime or to the viscous “undercooled” regime

between T_g and the recrystallization temperature of the glass, T_x. The convection inside the sample in terrestrial measurements is another problem.[25] In this work, we will use molecular dynamics simulation to investigate the temperature dependence of the viscosity and self-diffusion coefficients, as well as their relationship.

In Meyer's work,[16] the breakdown of the SE relation occurs in a Zr-based system. We study a $Cu_{33.3}Zr_{66.7}$ binary alloy, which is also a Zr-based system. To our best knowledge, the transport properties in the context of the SE relation of this alloy have not been reported previously. We hope that we can elucidate the mechanism for the breakdown of SE relation far above T_c and even the liquidus temperature based on the simulated transport properties, and propose an empirical way to predict the onset for this breakdown, which could also be applied to other systems.

There are several molecular dynamics studies of liquid and amorphous CuZr in various compositions, using different interaction models. Using a Lennard-Jones type interaction, plasticity was studied.[26] The structure and diffusion in $Cu_{60}Zr_{40}$ was studied using a Finnis-Sinclair interaction.[27] A tight binding based description was used in a study of amorphisation.[28] Kim and Lee developed a modified embedded atom model and gave a few results for $Cu_{50}Zr_{50}$.[29] Cheng *et al.* developed an embedded atom model and studied the structure basis of the mechanical properties of Cu_xZr_{100-x} (x=46 to 65).[30]

We simulate the CuZr system using a modified embedded atom model (MEAM) developed earlier. It has been used extensively in studies of the atomistics of diffusion. The typical chain-like structure of the diffusional motion, seen earlier in the glassy state,[31] was also found in the undercooled melt.[32] The observation of atomic jumps over nearest neighbor

distances coupled with the, often observed, time evolution of a secondary peak in the autocorrelation function led to the assumption of two distinct mechanisms, jumps over typically nearest neighbor distances and a more flow-like motion.[33] A detailed study of the atomic jump lengths showed that there is no typical jump length and that the long range jumps are just special cases of the collective jumps.[34] The evolution of the side maximum in the autocorrelation function is not due to the jump process but results from the prolonged waiting time between jumps at preferred sites.[35] This is an effect of the dynamic heterogeneity, implying faster atoms moving in a slower surrounding.

Recently Mendelev and coworkers developed another Finnis-Sinclair type potential for CuZr.[36] They had used previously a slightly different version to study diffusion.[37] An accurate assessment of the relative merits of this model compared to our MEAM is not possible. The predicted positions of the nearest neighbor peaks of the pair correlation functions differ by about 5%. Our MEAM gives 0.303, 0.244 and 0.3nm, for ZrZr, CuCu and ZrCu, respectively. The corresponding values for the EAM2 interaction are 0.321, 0.258 and 0.28nm. Reported experimental values are 0.318, 0.253 and 0.277nm,[38] 0.316, 0.257 and 0.284nm[39] and 0.316, 0.253 and 0.280 nm.[40] The ZrZr and CuCu values are fairly close to the experimental values for the mono-atomic melts. At T=1373K the position of the first peak is at 0.250nm for Cu[41] and at T=2000 at 0.312nm for Zr.[42] These slight discrepancies indicate limitations of the model description which, however, are not sufficient to severely affect the results of this investigation.

The organization of the rest of the paper is as follows. In the next section, we describe the system studied and the applied simulation methods. The results of the simulation are given

in Sect. III. Self-diffusion coefficients, viscosity, auto-correlation functions and heterogeneity are presented and discussed. Based on the simulated data, the breakdown of the Stokes-Einstein relation is shown. An empirical way to predict the breakdown of the SE relation is proposed, and the mechanism for the breakdown of SE relation is analyzed by the non-Gaussianity parameter. In Sect. IV the results are discussed in the context of our previous and that of other groups. We end with a summary in Sect V.

II. SIMULATION DETAILS

The molecular dynamics simulations are performed for systems of 1000~8000 atoms with periodic boundary conditions in three directions. The velocity Verlet algorithm is adopted to solve the equation of motion at constant temperature T and constant pressure P, and with a time step of 2.5fs. The pressure is kept zero using the Parrinello-Rahman algorithm [43] with a volume mass of $\sqrt{N} \cdot m_{Zr}$, where N is the number of particles and m_{Zr} is the atomic mass of Zr, and an additional damping term to prevent oscillations. The temperature T was controlled by a Nose-Hoover thermostat. [44]

Three independent samples are prepared by a quench from liquid $Cu_{33.3}$ $Zr_{66.7}$ at 2500K to 1200K, in steps of 100K and with a rate of 1×10^{12}K/s. Within the covered temperature range the system is in the equilibrium state. At each temperature step, the samples are aged for 2.5ns. This procedure followed our previous work. [45] In the temperature range relevant for the present investigation no aging effects are expected. [46] The measurements are taken during times ranging from 5ns at temperatures above 2000K, 15ns for temperatures below 1400K, and 10ns for the intermediate temperatures. The radial distribution functions at the beginning of the measurements, g_{r1}, and the end, g_{r2}, are calculated. The condition $g_{r1}=g_{r2}$ is always

ensured. During the whole time needed to gain the necessary statistics no change of the structure of the liquid is observed.

A. Atomic interaction potential

The atomic interaction in the $Cu_{33.3}Zr_{66.7}$ alloy is described by a modified-embedded-atom method (MEAM), [47] which can be viewed as the original embedded atom method (EAM) plus the additional angular correction. In the original EAM, the total energy of the system is described by a pair potential φ_{ij} and an embedding energy $F(\rho_0)$ which accounts for the additional many body effects due to the electronic density:

$$E_{pot} = \sum \varphi_{ij}(r_{ij}) + \sum_{i=1}^{N} F(\rho_{0,i}), \tag{2}$$

where r_{ij} is the distance between atom i and j, and $\rho_{0,i}$ is the electronic density of atom i, which is given by a superposition of radial functions $f(r)$

$$\rho_{0,i} = \sum_{\substack{j=1 \\ j\neq i}}^{N} f(r_{ij}). \tag{3}$$

To account for covalency, there is an additional angular correction in this work for Zr as apex atom, and the density takes the form

$$\rho_i = \rho_{0,i} \cdot \exp\left[\frac{1}{\rho_{0,i}^2} c \sum_{\substack{j,k=1 \\ j\neq i \\ k\neq i}}^{N} \cos^3(\Theta^{jik}) f_3(r_{ij}) f_3(r_{ik})\right], \tag{4}$$

where Θ^{jik} is the angle between $\vec{r}_{ij}$ and $\vec{r}_{ik}$, and $f_3(r)$ is the radial function in the angular correction term. An exponential plus additional term is used for both $f(r)$ and $f_3(r)$. The parameters were fitted to reproduce the experimental values of Cu, Zr and $CuZr_2$ crystals. The universal energy-volume relation of Rose *et a*l. [48] was used to determine the anharmonic

contributions, not sampled in the crystal but of essential importance in the disordered glassy state. We get lattice parameters a=0.363, a=0.323 and c=0.516, and a=0.338 and c=10.35nm (experimental values [49] a=0.362, a=0.323 and c=0.515, and a=0.322 and c=11.18nm) for Cu, Zr and $CuZr_2$ respectively. The $CuZr_2$ lattice is slightly distorted. The atomic volume, however, is only 2% too large. The sublimation and vacancy formation energies for Cu and Zr crystals agree with experiment. The enthalpies of fusion per atom relative to the monoatomic crystals are reproduced for the CuZr and $CuZr_2$ crystals within a few percent. Additionally the phonon dispersion curves and elastic constants of the mono-atomic lattices were used. In the case of Cu, excellent agreement was achieved. In Zr we get an overall agreement with experiment but some phonons deviate up to 30%, similar to other work. [50, 51] The detailed form and the parameters are given in our previous work. [45] For more details on the fitting procedure see Ref. 52.

B. Self-diffusion coefficient calculation

The self-diffusion coefficients *D* are calculated for Cu and Zr from the long time evolution of the respective mean-square displacements (MSD) , [53]

$$\left\langle r^2(t)\right\rangle = \frac{1}{N}\sum_{i=1}^{N}\left[r_i(t) - r_i(0)\right]^2 , \tag{5}$$

by the standard expression

$$D = \lim_{t\to\infty}\frac{1}{6t}\left\langle r^2(t)\right\rangle \tag{6}$$

where the bracket denotes the ensemble average and the sum is over all atoms of Cu and Zr, respectively.

Since the present study is concerned with temperatures well above the glass transition, no

problems with aging effects or long time plateaus in the MSD are encountered.

C. Viscosity calculation

The shear viscosity of a liquid is related to the fluctuations of the off-diagonal elements of the stress tensor. According to the Green-Kubo equation, [53] η can be calculated from an equilibrium simulation by a time integral over the stress auto-correlation function $\eta(t)$

$$\eta = \int_0^{+\infty} \eta(t)dt \,, \tag{7}$$

with

$$\eta\,(\,t) = \frac{1}{k_B TV}\left\langle \sigma^{xy}(t)\cdot\sigma^{xy}(0)\right\rangle, \tag{8}$$

where V is the volume of the system, T the temperature, k_B the Boltzmann's constant, and σ^{xy} is the component of the stress in xy direction, which can be computed from the velocities and the viral

$$\sigma^{xy} = \sum_i m_i v_i^x v_i^y - \sum_i \sum_{j>i} \frac{\partial \varphi(r_{ij})}{\partial r_{ij}} \frac{r_{ij}^x r_{ij}^y}{r_{ij}} \tag{9}$$

Isotropy of the liquid implies equality of all shears. In finite systems this is slightly violated and one averages over the different shears, indicated by the brackets in Eq. (8). For the calculation of the stress auto-correlation function $\eta(t)$, we utilize the method of overlapping-time-interval correlation averages suggested by Rapaport. [54] There are three quantities in this averaging method, namely, the duration of the MD simulation, t_D, the time window over which the stress autocorrelation function is computed, t_w, and the time interval between the start of successive windows, t_s. The number of time origins is related to these three quantities by

$$n_0 = 1 + \left[\frac{t_D - t_w}{t_s} \right], \tag{10}$$

where the bracket means the nearest integer value.

D. Incoherent intermediate scattering function

The transition from a simple liquid through undercooling to a glass is also seen in the incoherent intermediate scattering function

$$\Phi_A(q,t) = \left\langle \left\langle \exp\{iq[r_n(t) - r_n(0)]\} \right\rangle \right\rangle_{n \in A} \quad . \tag{11}$$

The double brackets indicate averaging over all atoms of type A (Cu or Zr) and over starting times t_0.

III. SIMULATION RESULTS

A. Mean square displacement (MSD) and diffusion coefficient

The calculated MSDs of Cu and Zr in liquid $Cu_{33.3}Zr_{66.7}$ at temperatures ranging from T=1200K to T=2400 are shown in Fig. 1. As usual, we observe three different regimes in the MSDs. For short times the MSDs are proportional to t^2, which is typical for vibration and ballistic motion of particles. For long times the diffusive regime is reached, MSD$\propto t$. At intermediate times a transient regime appears, i.e., plateau, between the ballistic and diffusive regimes when the liquid is cooled to below 1600K. With the decrease of the temperature, the plateau becomes more pronounced.

We evaluate the self-diffusion coefficients for Cu, D_{Cu}, and Zr, D_{Zr}, from the slope of the MSDs in the long-range diffusive regime. The results, averaged over the three samples, are presented in a double-logarithmic plot in Fig. 2, where the red solid symbols represent D_{Cu} and the blue solid ones D_{Zr}. The self-diffusion coefficients for the two species converted from

the viscosity via the Stokes-Einstein relation are also plotted in Fig.2, denoted by red and blue open symbols. We will come back to this later.

According to mode coupling theory (MCT), the temperature dependence of D_A is given by

$$D_A(T) = D_0^{MCT}(T - T_c)^{\gamma}. \quad (12)$$

Fitting the averaged self-diffusion coefficients of Cu and Zr to the above expression, we find, common to both components, T_c=1025K, and γ=1.52 and 1.93 for Cu and Zr, respectively. The MCT critical temperature T_c and the exponent γ_{Zr} are compatible with the earlier work [45], whereas γ_{Cu} lies between the value γ_{Cu}=1.34 derived from the diffusion coefficient and γ_{Cu}=1.57 derived from the intermediate scattering function. These values depend somewhat on the temperature range used in the fitting, and are, therefore, not exact. The different γ values for Cu and Zr indicate that the system should be described by a two-component-MCT. Weysser *et al.* have shown that even for a simple system of polydisperse quasi-hard spheres with Brownian dynamics the description by an effective monodisperse system breaks down in the $q \to 0$ limit. [55]

In many cases, for example in liquid Ni-Zr alloy [56] and a binary Lennard-Jones system, [57] the self-diffusion coefficients for the two species vary in parallel with changing temperature. In contrast, the diffusion coefficients for two species in the $Cu_{33.3}Zr_{66.7}$ melt diverge. To analyze this divergence of the diffusion coefficients in more detail, we calculate D_{Cu} / D_{Zr} and its first derivative $d(D_{Cu}/D_{Zr})/dT$. The results are illustrated in Fig. 3. Clearly, at temperatures above T~1700K, D_{Cu}/D_{Zr} increases as temperature decreases with a small constant rate of 3.4×10^{-4} / K. We refer to this regime as "near-parallel regime", where diffusion coefficients for two species run nearly parallel to each other. This behavior is

expected when the two species merely differ in their respective effective diameter, d in Eq. (1). At temperatures below 1600K, $d(D_{Cu}/D_{Zr})/dT$ changes almost linearly with temperature. In this regime the slope is around 50 times larger than that in the near-parallel regime. The difference between the diffusion coefficients for the two species increases rapidly and the divergence becomes more and more pronounced with decreasing temperature.

B. Incoherent intermediate scattering function $F_s(q, t)$

In Fig. 4, we present the incoherent intermediate scattering functions $F_s^{\alpha}(q,t)$ for the two components as a function of time. The wave numbers used for the two plots correspond to the location of the first maximum in the structure factor for Cu and Zr, respectively (q=2.66Å^{-1} for Cu, and q =2.55 Å^{-1} for Zr [46]). At short times, $F_s^{\alpha}(q,t)$ shows a Gaussian-type dependence on time, consistent with the ballistic motion of the particles in Fig. 1. At high temperatures, $F_s^{\alpha}(q,t)$ decays to zero on a picosecond time scale. At low temperatures, a small shoulder appears, which corresponds to the so-called β-regime, due to the cage effect, and to the corresponding plateau in the MSD. The decay from the end of the initial decay due to ballistic motion of the particle at high temperatures or from the end of the β-regime is called α-relaxation.

In the late α-relaxation regime $F_s^{\alpha}(q,t)$ can be well approximated by a Kohlrausch –Williams –Watts (KWW) function

$$F_s(q,t) = f_q \exp\left[-(\frac{t}{\tau_q})^{\beta_q}\right] \tag{13}$$

with an exponent β_q <1 and f_q<1.

Depending on the temperature, we use $F_s^{\alpha}(q,t)$ for times longer than 0.2~1.5ps to fit the

KWW stretched exponential function. In the considered temperature range β is independent of temperature, β_q^{Cu} = 0.697±0.039, and β_q^{Zr} = 0.82± 0.028. The increase of the α-relaxation time with decreasing temperature is depicted in Fig.5. Mode coupling theory predicts that the α-relaxation time is related to T_c by

$$\tau(T) = \tau_0 (T - T_c)^{-\gamma} \tag{14}$$

Data regression shows that the parameters of T_c=1025K, γ_{Cu}=2.21, and γ_{Zr}=2.39 could fit the data for temperatures below 2000K quite well. This value of T_c is the same as derived above from the self-diffusion coefficients. The exponents γ, however, are considerably higher than the ones derived from the diffusion coefficients.

If diffusion and α-relaxation are two expressions of the same process the product of self-diffusion coefficients and α-relaxation time should be constant, independent of temperature. Fig. 6 shows the product, $D\tau_\alpha$, against temperature. At high temperatures $D\tau_\alpha$ is almost a constant for both Cu and Zr. Below 1700K it increases rapidly. The relaxation slows down more rapidly than the diffusion. At 1200K the product of the α-relaxation time and self-diffusion coefficient is about a factor of 2, for Zr, or 3, for Cu, higher than at high temperatures. Thus, when the temperature decreases to below 1700K, the self-diffusion coefficients decouple from the α-relaxation time.

C. Shear viscosity

The stress auto-correlation functions (SACF) of $Cu_{33.3}Zr_{66.7}$ have been evaluated according to Eq. (8). The normalized SACFs, $<\eta(t)/\ \eta(0)>$, are shown in Fig. 7 for temperatures ranging from 2400K down to 1200K. The SACF decays rapidly towards zero as the correlation time increases. For longer times, e. g. longer than 2.0 ps for 2400K or 0.15 ns for 1200K, the

normalized SACF oscillates weakly around zero. We cut off the contribution of the SACF to the viscosity at that time step where the slowest normalized SACF of the three samples drops to below 8×10^{-4}. Another significant feature of the SACFs evolves at temperatures below 1600K, namely a bump in the correlation time-range of 0.3 ps to 0.4 ps. This bump is the effect of the boson peak vibrations, present in all glasses and still observable in undercooled liquids. The bump becomes more and more pronounced with a further decrease of temperature. In the intermediate scattering function, Fig. 4, the corresponding bump can be seen at the lowest temperatures.

In the viscosity calculation we choose the times t_D, t_w and t_s, according to two principles. First, the viscosity must approach its asymptotic value when the integration time reaches t_w. For this, t_w should be long enough to capture the decay of autocorrelation function in its entirety but not so long that noise is added to the correlation signal when the noise of correlation function approaches its intrinsic value. [58] Secondly, each independent off-diagonal stress tensor provides an independent estimate of the shear viscosity. Because in real fluids the shear viscosity is isotropic, these three independent estimates of the viscosity must converge to one single value. To monitor the convergence of the viscosity we introduce, following Ref. 57, an error ξ:

$$\xi = \frac{1}{\eta_{ave}}\sqrt{\frac{(\eta_{xy}-\eta_{ave})^2+(\eta_{xz}-\eta_{ave})^2+(\eta_{yz}-\eta_{ave})^2}{3}}, \qquad (15)$$

where η_{ave} is the arithmetic mean of the three independently determined viscosity estimates η_{xy}, η_{xz} and η_{yz}. According to the abovementioned two principles, t_w ranges in our simulation from 3ps to 150ps depending on temperatures. Taking t_D=5-15ns and t_s=10fs, we have a total of 5×10^5 -1.5×10^6 time origins.

The viscosities of $Cu_{33.3}Zr_{66.7}$ at 1800K calculated from the three off-diagonal stress tensors and the error ξ are presented in Fig. 8. It can be seen that the viscosity from each off-diagonal stress tensor shows an asymptotic behavior. The convergence of these three estimates of the shear viscosity is very good; the convergence error is less than 2% when the correlation time attains t_w. At the other temperatures the behavior is similar. The convergence errors at different temperatures are shown in Fig. 9. At temperatures above 1300K, ξ is less than 5%, and there seems to be no correlation between temperature and convergence error. At the lowest covered temperature 1200K the convergence error of 6.3% is still acceptable.

The viscosities from the three independent samples used in this work should converge to one single value for each temperature. To check this point, we present in Fig. 10 the viscosities for the three samples (A, B and C) separately. These results are consistent with each other, and their difference is less than 4%. This again confirms the good convergence of the viscosity calculation in our work.

The temperature dependence of the calculated viscosities for the three samples is given in Fig. 11. The averaged viscosity can be fitted by the MCT power law (blue line)

$$\eta(t) = \eta_0^{MCT}(T - T_c)^{-\gamma}. \tag{16}$$

For the viscosity the MCT power law only holds at temperatures below 1900K, which is consistent with MCT and similar to the case of α-relaxation time. The fit gives T_c=1042K, and γ=1.88. T_c is not far from the value gained from the self-diffusion coefficients and α-relaxation times (T_c = 1025K). The value of γ is very close to that derived from D_{Zr} (γ=1.93), but deviates strongly from the values derived from D_{Cu} (γ=1.52), and the α-relaxation times (γ=2.21 for Cu, and 2.39 for Zr).

The temperature dependence of the viscosity can also be fitted by a Vogel-Fulcher – Tammann (VFT) law [59-61] (red line in Fig. 11)

$$\eta(t) = \eta_0^{VFT} \exp\left(\frac{B}{T - T_0}\right). \tag{17}$$

The VFT law can describe the temperature dependence of the viscosity quite well in the whole simulated temperature range. Data regression gives B=2258K, and T_0=767K.

D. Size effect

In order to check for a possible size effect of the MD calculations, we did some tests for a system of 8000 atoms at several temperatures. The initial configuration is obtained by doubling one configuration of 1000 atoms in each dimension. The new configuration is run for 5 ns to equilibrate, and subsequently for 10ns to obtain the needed statistics. The normalized stress tensor autocorrelation functions for two system sizes at 1800K are presented in Fig. 12. The insert gives an enlargement of the curves from 1ps to 10ps. Clearly, the results for the two sizes of system are in excellent agreement. The dependence of the integrated shear viscosity on correlation time is illustrated in Fig. 13 for the two systems sizes. The viscosity gained from the 1000-atom-system agrees within 0.5% with the one gained from the larger system. There is no apparent improvement in the viscosity calculation as the system size increases. Therefore, we can say that there is no obvious size effect in our viscosity calculation, and the 1000-atom-system gives reasonable results. To improve the accuracy of the viscosity calculation, the length of the MD run is more important than the system size. This agrees with earlier results for a Lennard-Jones system. [20] There also no obvious size effect in the calculation of self-diffusion coefficients was reported.

E. Stokes-Einstein relation

From the Stokes-Einstein relation (Eq. 1) with "slip" boundary condition, the effective diameter for the particle, d_{SE}, can be written as

$$d_{SE} = \frac{k_B T}{2\pi\eta D} \quad . \tag{18}$$

As long as d_{SE} is a constant, independent of temperature, the SE relation is deemed to hold, otherwise, the SE relation has broken down. Besides the Stoke-Einstein diameters for the two components, we define an average diameter corresponding to the average diffusion coefficient, given by $D_{aver.}^{-1} = 0.333 D_{Cu}^{-1} + 0.667 D_{Zr}^{-1}$. Fig. 14 depicts the temperature dependence of the effective diameters for D_{Cu}, D_{Zr}, and $D_{aver.}$. Apparently, for these three diffusion coefficients, the effective diameter d_{SE} fluctuates around a value d_0 at temperatures above T^*. d_0 = 0.306nm for Zr, d_0 = 0.205nm for Cu, and d_0 = 0.276nm for the average. However, the d_{SE} start to deviate from their respective d_0 at a temperature of T^*~1600K for Zr and the average, and T^*~1900K for Cu. The self-diffusion coefficients for the two species, $D_{d0,\,SE}$, derived from the viscosity via the SE relation with d_0 as the effective diameter are shown in Fig.2. As expected at temperatures above T^* the $D_{d0,SE}$ agree well with their counterparts calculated from the MSD, whereas they deviate increasingly when the temperature drops below T^*.

To relate the effective diameters to the nearest neighbor structure, we calculate the partial radial correlation functions of $Cu_{33.3}Zr_{66.7}$ at different temperatures, see Fig.15. The first nearest neighbor distance of Zr-Zr is d_1^{Zr}=3.03Å, and that of Cu-Cu is d_1^{Cu} =2.44 Å, both nearly independent of temperature. The effective diameter for Zr approximated from the SE relation using slip boundary condition, d_0^{Zr}, agrees well with the nearest neighbor distance of the Zr-Zr pairs, d_1^{Zr}. For copper, d_0^{Cu} is 16% less than d_1^{Cu} .

From self-diffusion, viscosity, and α-relaxation time, we found a MCT T_c around 1030K. This T_c is far below the temperature T^*, where the SE relation breaks down for Zr as well as for Cu. This means that in the $Zr_{66.7}Cu_{33.3}$ binary melt the SE relation does not hold even at temperatures far above T_c. The temperature T^* is even higher than the simulated melting temperature T_L=1478K, which is calculated following a procedure described in the APPENDIX. This finding is contrary to experimental indications that the SE relation holds at temperatures above the mode coupling T_c but breaks down at temperatures below T_c. [10-13] However, the behavior of SE relation described in this work is quite similar to the experimental findings of Zr-Ti-Cu-Ni-Be melt. [16] In that work, the mobility of Ni and Ti atoms remains decoupled from viscous flow even above the liquidus temperature. This indicates that the breakdown temperature is material dependent and not simply determined by a single component mean field picture.

It has been suggested that the breakdown of the SE relation is related to a changeover from flow motion to more hopping like motion. [17] Such a changeover would most likely affect the diffusivities of the two constituents differently. To test this we calculated the ratio D_{Cu}/D_{Zr} and show in Fig. 14 the temperature derivative $d(D_{Cu} / D_{Zr})/dT$. It shows a similar temperature dependence as for the SE-radius of Zr. A larger $d(D_{Cu} / D_{Zr})/dT$ means a more rapid change of D_{Cu} / D_{Zr} with temperature, and a more rapid increase of the divergence of the two diffusion coefficients. It does not, however, explain the drop of the SE-diameter of Cu at even higher temperatures. We will come back to this point further down.

We test the universality of this argument by reproducing the data of the viscosity and the self-diffusion coefficient from the MD simulation of Bordat *et al.* [17] for a binary

Lennard-Jones system. In that work the SE relation breaks down at a temperature around 1.2, which is far above the MCT critical temperature T_c=0.435. In Fig. 16, we present the calculated values of $T/(2\pi D\eta)$ for the two species, D_2/D_1, and its first derivative $d(D_2/D_1)/dT$ based on the published data. Obviously, the first derivative of D_2/D_1 changes its temperature behavior at around a temperature of 1.2, which is exactly the temperature of the breakdown of the SE relation. Therefore, a "near-parallel" to "non-parallel" transition also occurs in the self-diffusion coefficients of the L-J liquid, and this transition in the diffusion mechanism is accompanied by the breakdown of SE relation. The hypothesis that the divergence behavior of diffusion coefficients is related to the breakdown of SE relation and that $d(D_2/D_1)/dT$ can predict the onset of the breakdown is confirmed .

F. Dynamic Heterogeneity

The breakdown of the SE-relation has often been linked to the evolution of the dynamic heterogeneity (DH), one of the characteristics of the glassy state. DH means that at any given time some atoms are more mobile than the average, but in the long time average equal mobility is restored. One of the standard measures of the DH is the non-Gaussianity parameter, $\alpha_2(t)$, [62]

$$\alpha_2(t) = \frac{3 < \Delta r^4(t) >}{5 < \Delta r^2(t) >^2} - 1 \tag{19}$$

where <···> denotes the average over all atoms of one species, and over start times t_0, $\Delta r^2(t)$ and $\Delta r^4(t)$ are the mean square and quartic displacements, respectively.

In a completely isotropic system $\alpha_2(t)=0$ for vibrations and diffusion. In the other limit where a single atom is mobile and all others immobile $\alpha_2(t)=\infty$ for $t=\infty$. Generally, $\alpha_2(t)$ starts at

zero and increases in the ps range to values of the order of 0.1 due to anisotropies in vibration or short distance ballistic-like motion. It then increases $\propto \sqrt{t}$ towards a maximum and finally decays approximately $\propto 1/t$. [63] The $\sqrt{t}$ increase has been explained by the collectivity of motion. With decreasing temperature the maximum value of $\alpha_2(t)$ increases and is reached later.

The $\alpha_2(t)$ for Cu and Zr for different temperatures are illustrated in Fig. 17. They agree with the ones reported earlier, mainly at low temperatures. [45] Their behavior is similar to the one observed in other liquids. [63, 64] At high temperatures, as expected, $\alpha_2(t)$ reaches a weak maximum on a ps timescale. As the temperature is lowered the DH of the melt becomes more and more pronounced, and the maximal non-Gaussianity parameter, α_2(MAX), is reached later and later. At T=1200K, $\alpha_2(t)$ grows for about 20ps and its maximal value is increased by an order of magnitude To show the temperature dependence of dynamics heterogeneity more clearly, the α_2(MAX) at different temperatures for the two species and their first derivatives with respect to temperature, dα_2(MAX)/dT, are reported in Fig. 18. The temperature dependence of dα_2(MAX)/dT shows the same trend as d(D_{Cu}/D_{Zr})/dT, and as the effective diameter of the SE relation, d_{SE}. At temperatures above 1800K, dα_2(MAX)/dT is nearly constant, whereas it decreases linearly at temperatures below 1500K. From the intersection of the linear approximations in the two regimes of dα_2(MAX)/dT the transition temperature is found at about 1600K. This temperature equals the one found for the change in slope of the temperature derivative of the ratio of the self-diffusion coefficients of the two species, see Fig.14. Below this temperature the DH of the liquid increases upon cooling with a much enhanced rate. Therefore, it is reasonable to say that the change of self-diffusion

coefficient ratio is accompanied by a sudden increase of the dynamic heterogeneity. And it is this sudden increase of the dynamic heterogeneity which results in the breakdown of the SE relation.

IV. DISCUSSION

The simulated $CuZr_2$ melt shows the typical features of glass forming systems when they are quenched from the simple liquid to the undercooled liquid state. The viscosity, α-relaxation time and diffusion coefficients can be fitted by the MCT with a single critical temperature T_c. The different values of γ for Cu and Zr indicate the limitations of a simple one-component MCT for our system. At the same time the atomic dynamics of Cu and Zr differ significantly. At T=1200K the diffusivity of Cu is four times that of Zr. This higher mobility transpires in several other properties such as the breakdown of the SE relation. The slower majority species Zr is considered to be the structure forming one. We expect, therefore, that some of the differences between the dynamics of Cu and Zr will depend strongly on the composition and might disappear for systems with a larger Cu concentration. Our results reflect in part typical features of metallic melts, mainly seen in the Zr results, but also some more system specific ones, seen in the differences of the results for Cu and Zr.

Concentrating on Zr we see a clear correlation between the onset of the rapid increase in dynamic heterogeneity and the breakdown of the SE relation. Such a correlation has been seen in simulations of several other materials and the DH was given as the reason for the breakdown. [18,19,21,65] If some atoms move fast they will give a large contribution to diffusion whereas viscosity is strongly influenced by the slow atoms. A simulation for high density hard sphere fluids has shown that the slow particles obey the SE relation. [18] We have seen the

correlation in the non-Gaussianity parameter α_2 which is dominated by the fast moving atoms. It would be interesting to test whether such a correlation can also be found in the alternate non-Gaussianity parameter γ, [66, 67] which is dominated by the slow atoms.

It has been suggested that the breakdown of the SE relation is due to a change in the nature of the atomic motion. Bordat *et al.* [17] ascribe the breakdown of the SE relation to the transition of flow motion to hopping motion when the system becomes aware of the underlying energy landscape. In particular hopping between sites, where the particles are localized for some time, is taken as an indication. In this work we find that the onset of the breakdown of the SE relation can be determined from the ratio of the diffusion coefficients of the two components, hinting towards a change in mechanism affecting the two components differently. Earlier we related the time dependence of the DH to the collectivity of the jump process in glasses and undercooled liquids. [63] Experiments and simulations have shown that diffusion in both the glass and the undercooled liquid is collective [7]. From the isotope effect of the diffusion coefficient in mono-atomic and binary Lennard-Jones liquids it has been shown that this collectivity grows far above the MCT critical temperature T_c. [68, 69] A study of the pressure dependence of the diffusion in the binary Lennard-Jones liquid has shown that the activation volume drops already at twice T_c from the value in the hot liquid V_{act} =0.6Ω (Ω=atomic volume) to the much lower value of V_{act} =0.3Ω which is an indication of correlated jump motion. [57] A detailed analysis of the atom motion in the present system has shown that there is no preferred jump length and the contribution of jumps over a nearest neighbor distance to the diffusion of Zr is small even at 1400K. [45] The distribution of jump lengths was found to be independent of temperature; the jump probability followed an Arrhenius law. These

simulation results indicate that there is indeed a change in the nature of the atomic motion already at temperatures far above T_c.

Affouard *et al.*[21] ascribe the violation of the SE relation to a decoupling between the A and B particles in a binary generalized Lennard-Jones system. They observe different SE breakdowns at different temperatures for the two components. A collective jump process, however, involves both species. The chain (or string) of jumping atoms involves them both, perhaps with a probability somewhat deviating from their concentrations. On the other hand, we also observe different breakdown temperatures for Zr and Cu in our system. A key to these different temperatures for Cu and Zr can be seen in the respective time evolutions of the van Hove pair correlation functions [35] and in particular in the time evolution of the self hole, i.e. the probability that the site of a given atom is taken by a different atom. In the long time limit, the self hole is filled with Cu and Zr atoms according to their concentration, independent of whether it starts as a Zr or Cu site. The site of a Zr atom is filled by another Zr atom approximately following a simple exponential law, as expected for normal diffusion. In contrast, the site of a Cu atom is filled first with an enhanced probability by another Cu atom, before the filling probability drops to the statistical average. This leads to the seemingly paradoxical result that the correlation function of the faster particle decays more slowly. This effect can be explained by the relative rigidity of the Zr-matrix enhanced by the dynamic heterogeneity in combination with the correlation between neighboring Cu atoms. This replacement of a Cu atom by another Cu atom contributes to tracer diffusion but has little effect on viscosity, since the surrounding need not change. An onset of this is already visible at T=2000K. It can explain the deviation from the SE relation for Cu diffusion at higher

temperatures than for Zr. We want to stress that this effect will be strongly concentration- and material-dependent. We do not expect that this latter effect occurs also in Cu rich CuZr melts.

V. SUMMARY

Using a modified embedded atom potential we calculated by molecular dynamics the shear viscosity, the intermediate scattering function, the tracer self-diffusion coefficients and the non-Gaussianity parameter of a $Cu_{33.3}Zr_{66.7}$ melt at temperatures from 1200K to 2500K. The shear viscosity is calculated from a Green Kubo relation. No system size dependence is observed. The diffusion coefficients are evaluated from the long time limits of the mean square displacements. Plotted against temperature, the self-diffusion coefficients of the two components diverge away from each other, whereas e. g. for binary Lennard-Jones melts they evolve nearly in parallel with temperature. Both the diffusion coefficients and the intermediate scattering functions can be fitted by MCT with a common critical temperature T_c ~ 1030K, in agreement with earlier work. The Stokes-Einstein relation between viscosity and diffusion coefficient starts to be strongly violated already at T~1600K, which is far above the MCT critical temperature and above the melting temperature. At the same temperature the dynamic heterogeneity starts to increase rapidly. At about the same temperature there is also a change of slope in the temperature derivative of the ratio of the two diffusion coefficients, $d/dt\ (D_{Cu}/D_{Zr})$. We relate the breakdown of the SE-relation to the dynamic heterogeneity which in turn is connected to a change in atomic motion.

For the diffusion of the minority component Cu the SE-relation breaks down at even higher temperatures. This additional effect can be traced to the much higher mobility which allows the replacement of a Cu atom, which has moved away, by another Cu atom before the

surrounding Zr-dominated matrix has changed its structure too much. This effect should be absent in the Cu rich CuZr melt, but should be observable for other small minority components in melts.

The breakdown of the SE relation even at temperatures above the melting temperature indicates that it should be used only with great caution to approximate the viscosity from the self-diffusion coefficients or vice versa.

ACKNOWLEDGEMENTS

We are grateful to A. Meyer and J. Horbach for their comments and suggestions. Financial supports from the National Natural Science Foundation of China (Grant Nos. 50371043 and 50890174), Shanghai Municipal Natural Science Foundation (Grant No. 10ZR1415700), and Research Fund for the Doctoral program of Higher Education of China (Grant No. 20100073120008) are acknowledged.

APPENDIX

Here we provide the simulation details of predicting the melting temperature for $CuZr_2$ with our MEAM potential.

For the prediction of the melting temperature, we use a coexisting structure of crystal and liquid. During the simulation, we use a NPT ensemble with the external pressure kept at zero using the Parrinello-Rahman algorithm. At the beginning, a $CuZr_2$ crystal of 1800 atoms with stable lattice structure is equilibrated for 1ns at 600K. The liquid phase is then generated by heating the well equilibrated solid phase to 2000K and equilibrating for 1ns. The two subsystems are merged together by joining them in the z-axis direction. Finally, the whole

system with a total number of 3600 atoms is allowed to evolve for 7.5ns (3,000,000 time steps) at given temperatures. The equilibrium melting temperature, T_L, is estimated from the change of the growth direction in the coexisting solid and liquid structure. At temperatures above T_L, the liquid phase will grow on the expense of the solid phase and vice versa at temperatures below T_L.

Fig. 19 presents the simulated potential energy per atom, E_{pot}, at its homogeneous end state at different temperatures when starting with a coexisting structure of solid and liquid. For the temperature dependence of the potential energy, there is an abrupt change between 1475K and 1482K. The change of the potential energy with time at these two temperatures is illustrated in Fig.20. Clearly, the coexisting structure crystallizes at 1475K but melts at 1482K. Therefore, the melting temperature of $CuZr_2$ lies between these two temperatures. We approximate T_L as $T_L^{simu.}$=1478.5±3.5K, which is close to the experimental value, $T_L^{exp.}$=1310K, the deviation being around 12.8%.

---

* Author to whom correspondence should be addressed. Email address: xjhan@sjtu.edu.cn

† Email address: H.Schober@fz-juelich.de

[1] M. H. Cohen, G. S. Grest, Phys. Rev. B **20**, 1077 (1979).

[2] Y. Yokoyama, T. Ishikawa, J. T. Okada, Y. Watanabe, S. Nanao, A. Inoue, J. Non-Cryst. Solids **355**, 317 (2009).

[3] L. Battezzati, G. S. Greer, Acta Metall. **37,** 1791 (1989).

[4] I. Egry, G. Lohöfer, I. Seyhan, S. Schneider , B. Feuerbacher, Appl. Phys. Lett. **73**, 462 (1998).

[5] A. Masuhr, T. A. Waniuk, R. Busch, and W. L. Johnson， Phys. Rev. Lett. 82, 2290 (1999).

[6] X. J. Han, M. Chen, and Y .J. Lv, Int. J. Thermophys. **29**, 1408 (2008).

[7] F. Faupel, W. Frank, M-P. Macht, H. Mehrer, V. Naundorf, K. Rätzke, H. R. Schober , S. K. Sharma, and H. Teichler, Rev. Mod. Phys. **75**, 237 (2003).

[8] H. J. V. Tyrrell and K. R. Harris, *Diffusion in Liquids* (Butterworths, London, 1984).

[9] U. Balucani and M. Zoppi, *Dynamics of the Liquid State* (Clarendon, Oxford, 1994).

[10] I. Chang and H. Sillescu, J. Phys. Chem. B **101**, 8794 (1997).

[11] V. Zöllmer, K. Rätzke, and F. Faupel, J. Mater. Res. **1**8, 2688 (2003).

[12] A. Meyer, Phys. Rev. B **66**, 134205 (2002).

[13] V. Zöllmer, K. Rätzke, F. Faupel, A. Meyer, Phys. Rev. Lett. **90**, 195502 (2003).

[14] W. Götze and L. Sjögren, Rep. Prog. Phys. **55**, 241 (1992).

[15] S. K. Das, J. Horbach, and T. Voigtmann, Phys. Rev. B **78**, 064208 (2008).

[16] A. Meyer, W. Petry, M. Koza, and M. –P. Macht, Appl. Phys. Lett. **83**, 3894 (2003).

[17] P. Bordat, F. Affouard, M. Descamps and F. Müller-Plathe, J. Phys.-Condens. Matt. **15**, 5397 (2003).

[18] S. Kumar, G. Szamel, and J. F. Douglas, J. Chem. Phys. **124**, 214501 (2006).

[19] R. Yamamoto, and A. Onuki, Phys. Rev. Lett. **81**, 4915 (1998).

[20] M. Cappelezzo, C. A. Capellari, S. H. Pezzin, and L. A. F. Coelho, J. Chem. Phys **126**, 224516 (2007).

[21] F. Affouard, M. Descamps, L.-C. Valdes, J. Habasaki, P. Bordat, and K. L. Ngai, J. Chem.

Phys. **131**, 104510 (2009).

[22] S. R. Becker, P. H. Poole, and F. W. Starr, Phys. Rev. Lett. **97**, 055901 (2006).

[23] J. Horbach, and W. Kob, Phys. Rev. B **60**, 3169 (1999).

[24] X.J. Han, B. Wei, Philos. Mag. **83,** 1511 (2003).

[25] D.M. Herlach, R.F. Cochrane, I. Egry, H.J. Fecht, A.L. Greer, Int. Mater. Rev. **38,** 273 (1993).

[26] A. C. Lund, and C. A. Schuh, Appl. Phys. Lett. **82**, 2017 (2003).

[27] Y. L. Sun, J. Shen, and A. A. Valladares, J. Appl. Phys. **106**, 073520 (2009).

[28] S.-H. Liang, J.-H. Li, and B.-X. Liu, J. Phys. Soc. Japan **77**, 104301 (2008).

[29] Y.-M. Kim, and B.-J. Lee, J. Mater. Res. **23**, 1095 (2008).

[30] Y. Q. Cheng, H. W. Sheng, and E. Ma, Phys. Rev. B **78**, 014207(2008).

[31] H. R. Schober, C. Oligschleger, and B. B. Laird, J. Non-Cryst. Solids **156**, 965 (1993).

[32] H. R. Schober, C. Gaukel, and C. Oligschleger, Prog. Theor. Phys. Suppl. **126**, 67 (1997).

[33] C. Gaukel, and H. R. Schober, Solid State Commun. **107**, 1 (1998).

[34] M. Kluge, and H. R. Schober, Phys. Rev. B **70**, 224209 (2004).

[35] M. Kluge, and H. R. Schober, J. Non-Cryst. Solids **352**, 5093 (2006).

[36] M. I. Mendelev, M. J. Kramer, R. T. Ott, D. J. Sordelet, D. Yagodin, and P. Popel, Phil. Mag. **89**, 967 (2009).

[37] M. I. Mendelev, M. J. Kramer, R. T. Ott, D. J. Sordelet, Phil. Mag. **89**, 109 (2009).

[38] H. S. Chen, and Y. Waswda, Phys. Stat. Sol. (a) **51**, 593 (1979).

[39] Yu. A. Babanov, V. R. Schvetsov, and A. F. Sidorenko, Physica B **208**, 375 (1995).

[40] N. Mattern, P. Jovari, I. Kaban, S. Gruner, A. Elsner, V. Kokotin, H. Franz, B. Beuneu and J.

Eckert, J. Alloy and Compounds **485**, 163 (2009).

[41] M. I. Mendelev, M. J. Kramer, C. A. Becker, and M. Asta, Phil. Mag. **88**, 1723 (2008).

[42] T. Schenk, D. Holland-Moritz, V. Simonet, R. Bellissent, and D. M. Herlach, Phys. Rev. Lett. **89**, 075507 (2002).

[43] M. Parrinello and A. Rahman, Phys. Rev. Lett. **45**, 1196 (1980).

[44] W. G. Hoover, Phys. Rev. A **31**, 1695 (1985).

[45] M. Kluge and H. R. Schober, Phys. Rev. B **70**, 224209 (2004).

[46] M. Kluge, *Molekulardynamik-Simulation der Diffusion in binären unterkühlten metallischen Schmelzen und Gläsern aus* $Cu_{33}Zr_{67}$, Ph. D thesis, Forschungszentrum Jülich, 2001.

[47] M. I. Baskes and R. A. Johnson, Modell. Simul. Mater. Sci. Eng. **2**, 147 (1994).

[48] J. H. Rose, J. R. Smith, F. Guinea, and J. Ferrante Phys. Rev. B **29**, 2963 (1984).

[49] E. Kneller, Y. Khan, and U. Gorres, Z. Metallkd. **77**, 43 (1986).

[50] F. Willaime and C. Massobrio, Phys. Rev. Lett. **63**, 2244 (1989).

[51] B. L. Zhang, C. Z. Wang, K. M. Ho, D. Turner, and Y. Y. Ye, Phys. Rev. Lett **74**, 1375 (1995).

[52] C. Gaukel, *Dynamics of Glasses and Undercooled Melts of Zr-Cu*, Vol. 3556 Berichte des Forschungszentrums Jülich, (Forschungszentrum Jülich, Germany 1998).

[53] M. P. Allen and D. J. Tildesley, *Computer Simulation of Liquids* (Clarendon Press, Oxford, 1987)

[54] D.C. Rapaport, *The Art of Molecular Dynamics Simulation* (Cambridge University Press, Cambridge, 1995)

[55] F. Weysser, A. M. Puertas, M. Fuchs, and Th. Voigtmann, Phys. Rev. E 82, 011504(2010).

[56] H. Teichler, Phys. Rev. Lett. **76**, 62 (1996).

[57] H. R. Schober, Phys. Rev. Lett. **88**, 145901 (2002).

[58] D. Nevins and F. J. Spera, Mole. Simul. **3**3, 1261 (2007).

[59] H. Vogel, Phys. Z. **22,** 645 (1921).

[60] G. S. Fulcher, J. Am. Ceram. Soc. **8,** 339 (1925).

[61] G. Tammann and G. Hesse, Z. Anorg. Allg. Chem. **156,** 245 (1926).

[62] A. Rahman, Phys. Rev. A **136**, 405 (1964).

[63] D. Caprion, J. Matsui, and H. R. Schober, Phys. Rev. Lett. **85**, 4293 (2000).

[64] W. Kob, C. Donati, S. J. Plimpton, P. H. Poole, and S. C. Glotzer, Phys. Rev. Lett. **79**, 2827 (1997).

[65] D. Bonn, and W. K. Kegel, J. Chem. Phys. **118**, 2005 (2003).

[66] E. Flenner, and G. Szamel, Phys. Rev. E **72**, 011205 (2005).

[67] E. J. Saltzman, and K. S. Schweizer, Phys. Rev. E **74**, 061501 (2006).

[68] M Kluge and H. R. Schober, Phys. Rev. E **62**, 597 (2000).

[69] H. R. Schober, Sol. State Commun. **119**, 1 (2001).

Figure Captions

FIG. 1. Log-log plot of the mean square displacements of Cu and Zr in liquid $Cu_{33.3}Zr_{66.7}$ at temperatures between 1200K and 2400K

FIG. 2. Self-diffusion coefficients of Cu (red) and Zr (blue) in liquid $Cu_{33.3}Zr_{66.7}$ against temperature. (Solid symbols: *D* calculated from the MSD, open symbols: *D* derived from the viscosity via the SE relation, lines: fit with the MCT expression). T_L indicates the calculated melting temperature

FIG. 3. D_{Cu}/D_{Zr} of liquid $Cu_{33.3}Zr_{66.7}$ and its first temperature derivative versus temperature for the three samples .

FIG. 4. Incoherent intermediate scattering function for Cu and Zr in liquid $Cu_{33.3}Zr_{66.7}$ at different temperatures (From left to right, the temperature changes from 2500K to 1200K with a step of 100K)

FIG. 5. α-relaxation time versus (T-T_c) for Cu and Zr in liquid $Cu_{33.3}Zr_{66.7}$ (symbols: this simulation, lines: fit with the MCT expression).

FIG. 6. Product of self-diffusion coefficient and α-relaxation time, $D\tau_\alpha$, for Cu and Zr in liquid $Cu_{33.3}Zr_{66.7}$ against temperature (symbols: this simulation, lines: guide to the eye).

FIG. 7. Normalized stress autocorrelation function of liquid $Cu_{33.3}Zr_{66.7}$ at different temperatures

FIG. 8. Viscosities, calculated from three independent off-diagonal stress tensors, and convergence error of liquid $Cu_{33.3}Zr_{66.7}$ at 1800K versus integration time

FIG. 9. Convergence errors of the viscosity calculation at different temperatures

FIG. 10. Viscosity of liquid $Cu_{33.3}Zr_{66.7}$ at 1800K from three independent samples of 1000 atoms each and one sample of 8000 atoms.

FIG. 11. Viscosity of liquid $Cu_{33.3}Zr_{66.7}$ against temperature (symbols: this simulation, red line: fit with the VFT expression, blue line: fit with the MCT expression).

FIG. 12. Normalized stress tensor autocorrelation function at 1800K for samples of 1000 (blue line) and 8000 (red line) atoms.

FIG. 13. Viscosity of liquid $Cu_{33.3}Zr_{66.7}$ at 1800K for samples of 1000 (blue line) and 8000 (red line) atoms.

FIG. 14. Effective SE diameters d_{SE}, calculated from D_{Cu}, D_{Zr}, and $D_{aver.}$, and $d(D_{Cu}/D_{Zr})/dT$.

FIG. 15. Pair correlation functions for Cu-Cu and Zr-Zr at different temperatures

FIG. 16. Effective diameters of the two species, ratio of their self-diffusion coefficients D_2/D_1, and its first derivative for a binary Lennard-Jones system, reproduced from Ref. 17. The effective diameter has the unit of σ_1, $d(D_2/D_1)/dT$ has the unit of k_B/ε_1, where k_B is the Boltzmann's constant, σ_1 and ε_1 are the length and energy parameter for the first component.

FIG.17. Non-Gaussian parameters for Cu and Zr in liquid $Cu_{33.3}Zr_{66.7}$ at different temperatures (from low to top, the temperature changes from 2500K to 1200K with a step of 100K)

FIG. 18. Maximum of the non-Gaussianity parameter α_2(MAX) and its first derivative for Cu and Zr liquid $Cu_{33.3}Zr_{66.7}$ against temperature

FIG. 19. Potential energy of the coexisting structure at different temperatures.

FIG. 20. Variation of potential energy for the coexisting structure during simulation at two different temperatures.

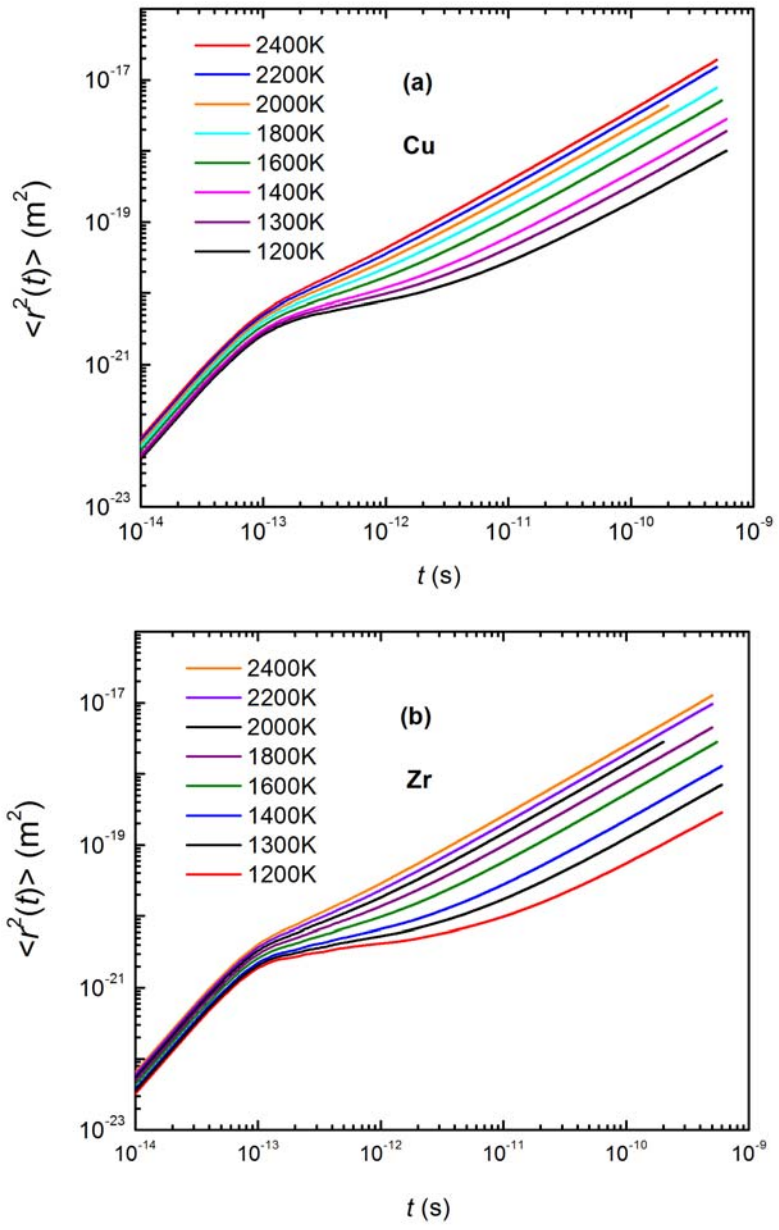

FIG. 1. Log-log plot of the mean square displacements of Cu and Zr in liquid $Cu_{33.3}Zr_{66.7}$ at temperatures between 1200K and 2400K

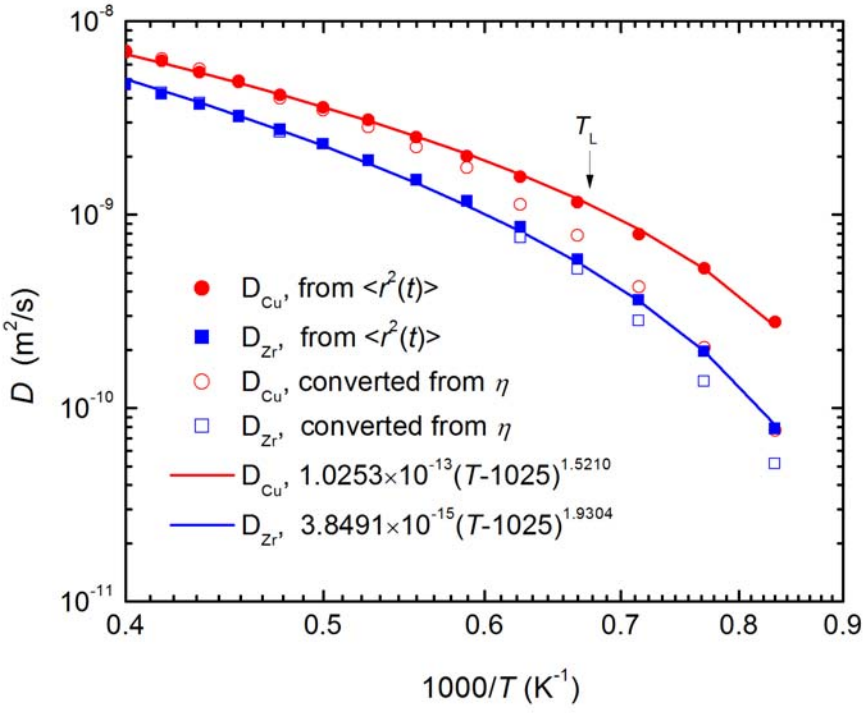

FIG. 2. Self-diffusion coefficients of Cu (red) and Zr (blue) in liquid $Cu_{33.3}Zr_{66.7}$ against temperature. (Solid symbols: *D* calculated from the MSD, open symbols: *D* derived from the viscosity via the SE relation, lines: fit with the MCT expression). T_L indicates the calculated melting

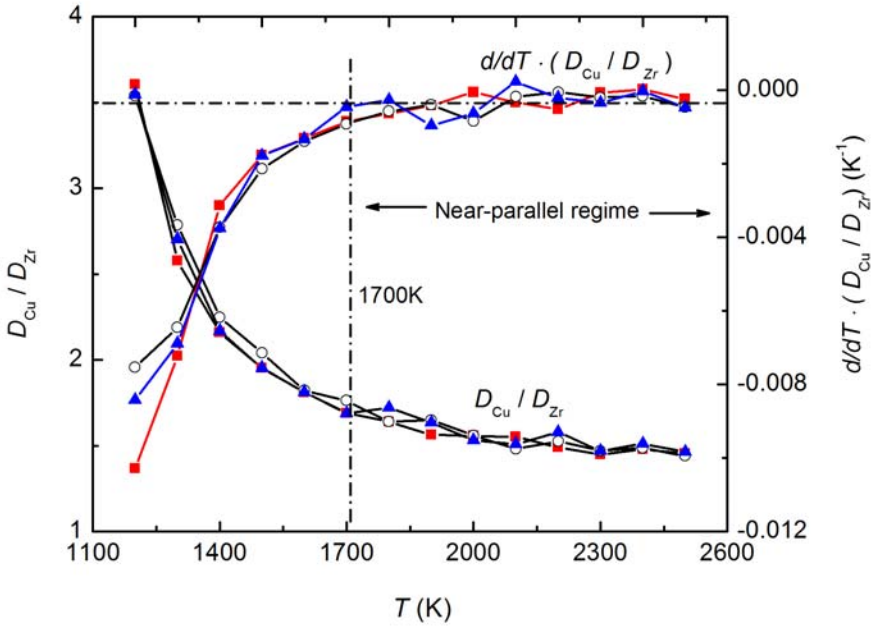

FIG. 3. D_{Cu}/D_{Zr} of liquid $Cu_{33.3}Zr_{66.7}$ and its first temperature derivative versus temperature for the three samples.

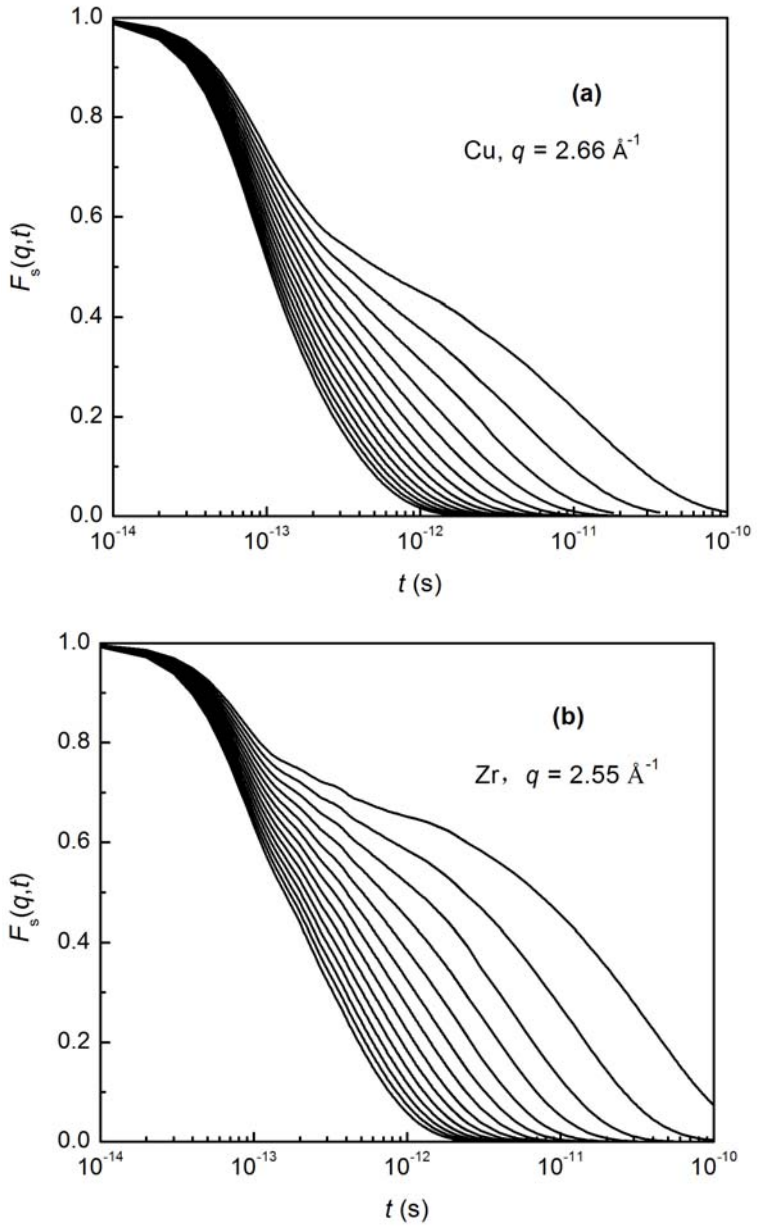

FIG. 4. Incoherent intermediate scattering function for Cu and Zr in liquid $Cu_{33.3}Zr_{66.7}$ at different temperatures (From left to right, the temperature changes from 2500K to 1200K with a step of 100K)

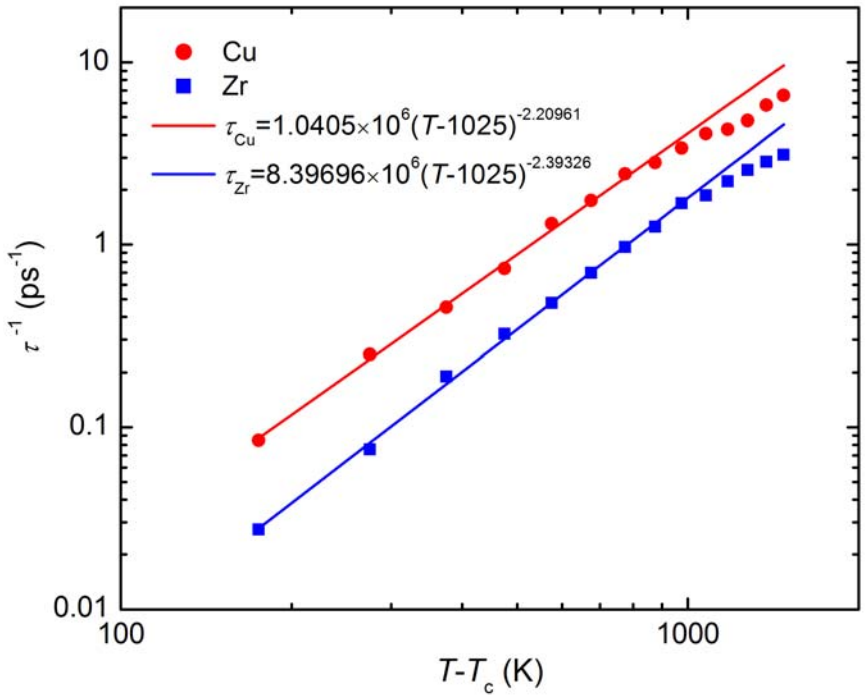

FIG. 5. α-relaxation time versus (T-T_c) for Cu and Zr in liquid $Cu_{33.3}Zr_{66.7}$ (symbols: this simulation, lines: fit with the MCT expression).

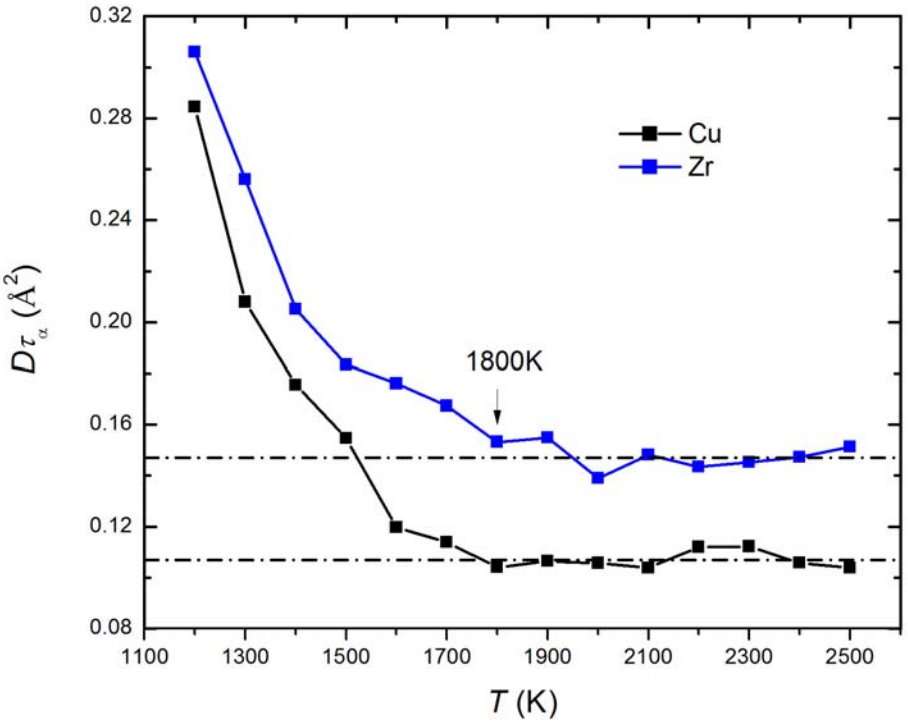

FIG. 6. Product of self-diffusion coefficient and α-relaxation time, $D\tau_\alpha$, for Cu and Zr in liquid $Cu_{33.3}Zr_{66.7}$ against temperature (symbols: this simulation, lines: guide to the eye).

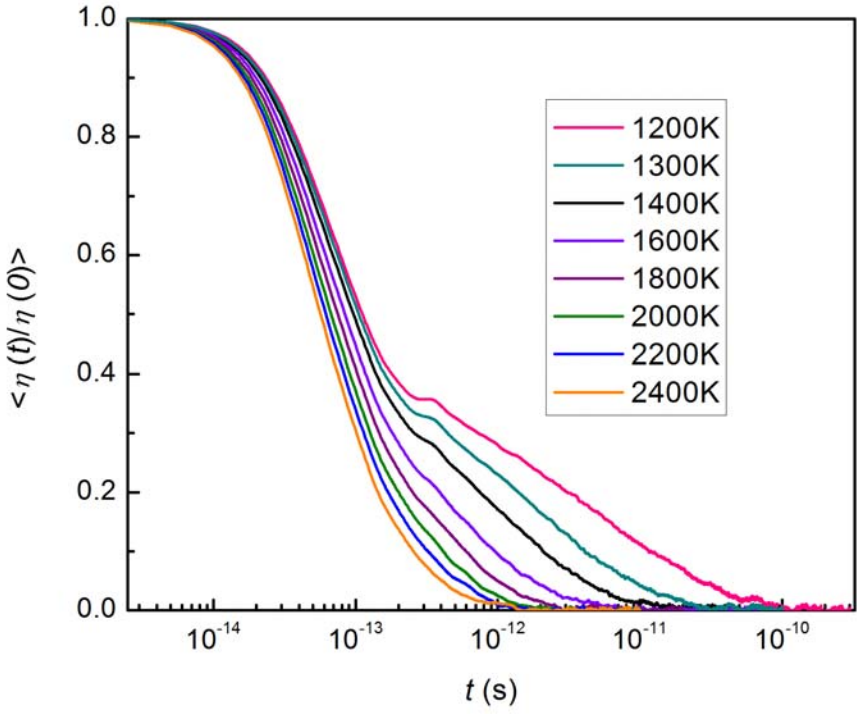

FIG. 7. Normalized stress autocorrelation function of liquid $Cu_{33.3}Zr_{66.7}$ at different temperatures

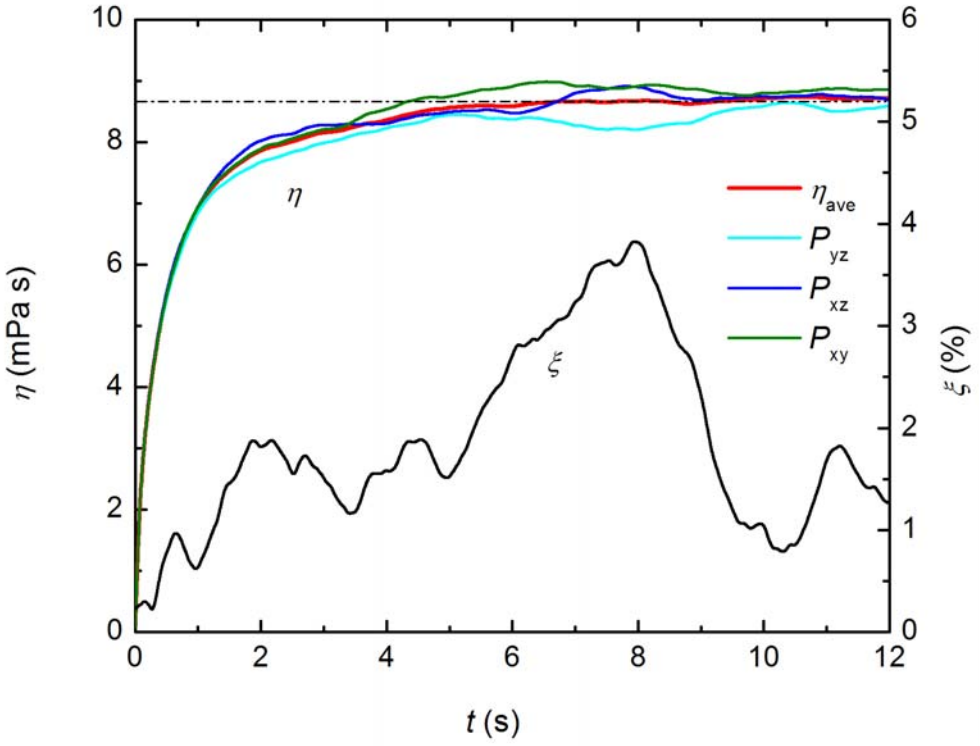

FIG. 8. Viscosities, calculated from three independent off-diagonal stress tensors, and convergence error of liquid $Cu_{33.3}Zr_{66.7}$ at 1800K versus integration time

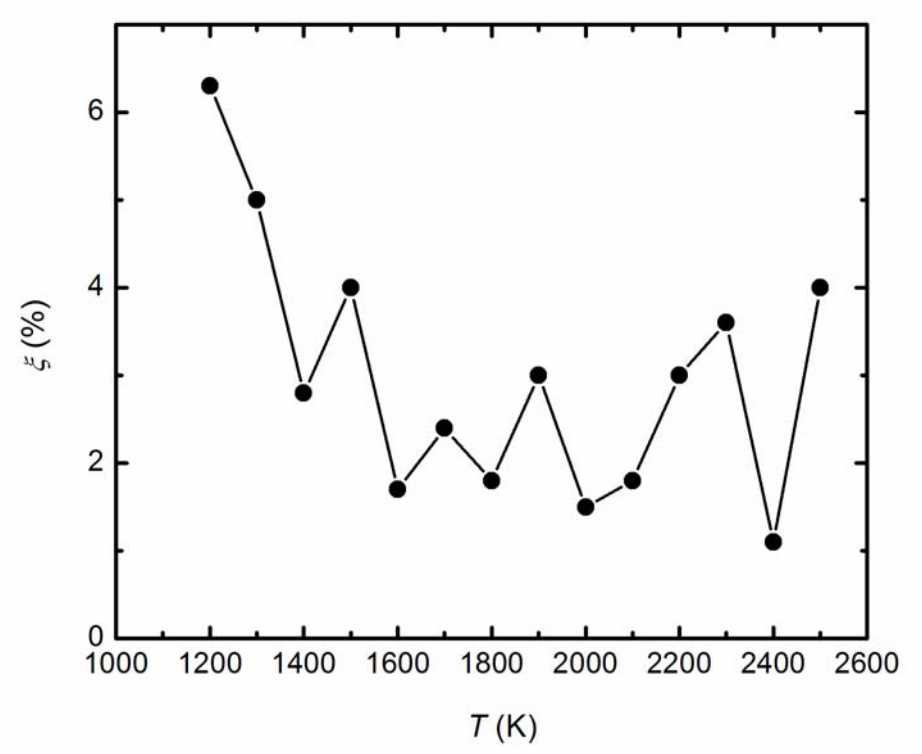

FIG. 9. Convergence errors of the viscosity calculation at different temperatures

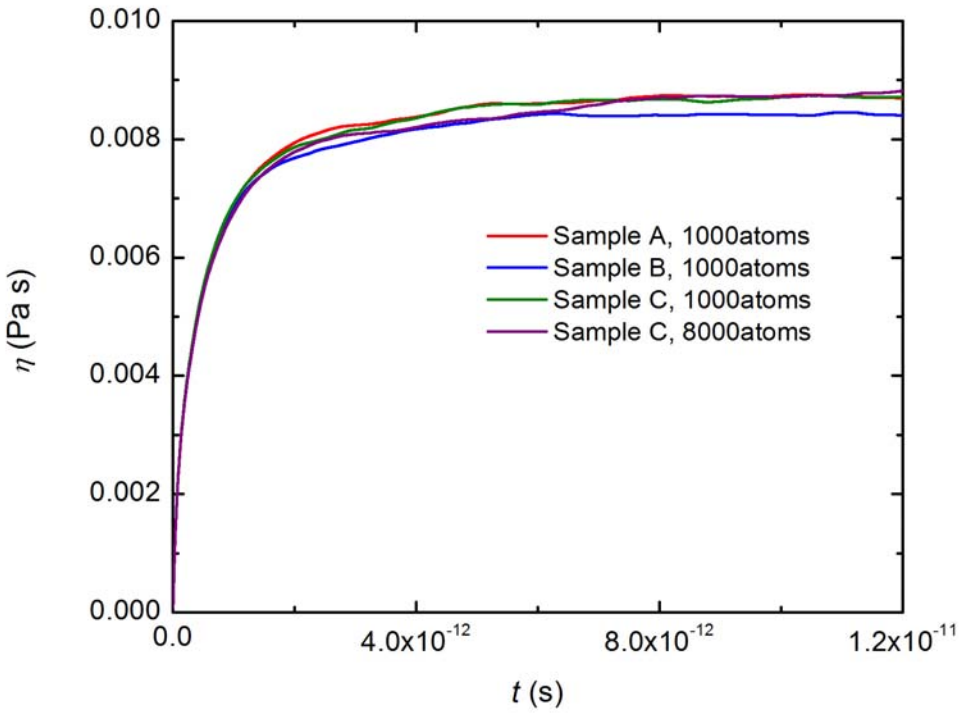

FIG. 10. Viscosity of liquid $Cu_{33.3}Zr_{66.7}$ at 1800K from three independent samples of 1000 atoms each and one sample of 8000 atoms.

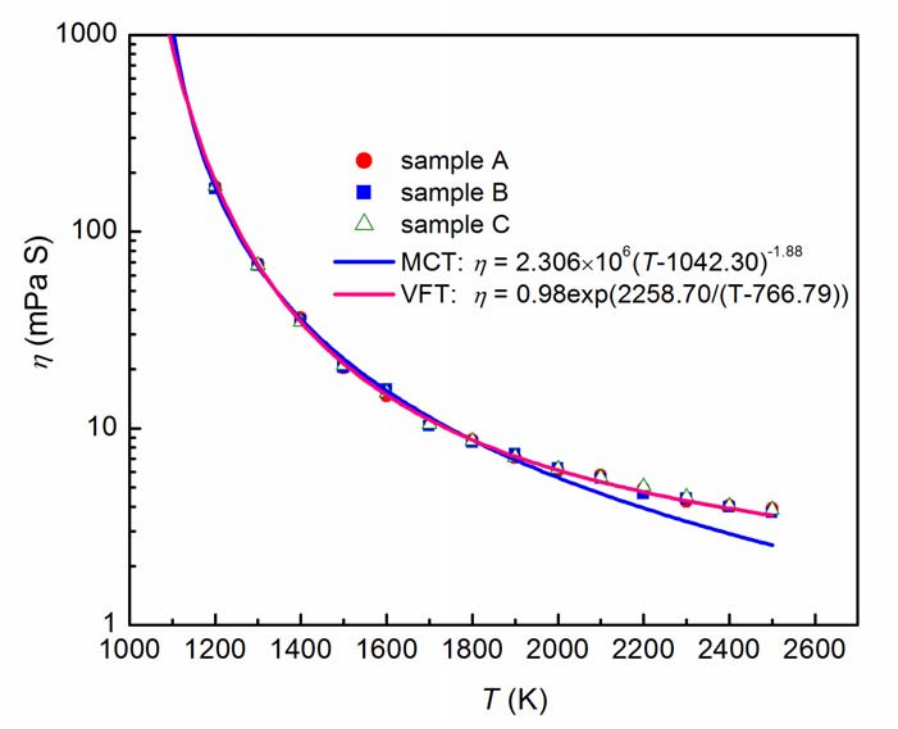

FIG. 11. Viscosity of liquid $Cu_{33.3}Zr_{66.7}$ against temperature (symbols: this simulation, red line: fit with the VFT expression, blue line: fit with the MCT expression).

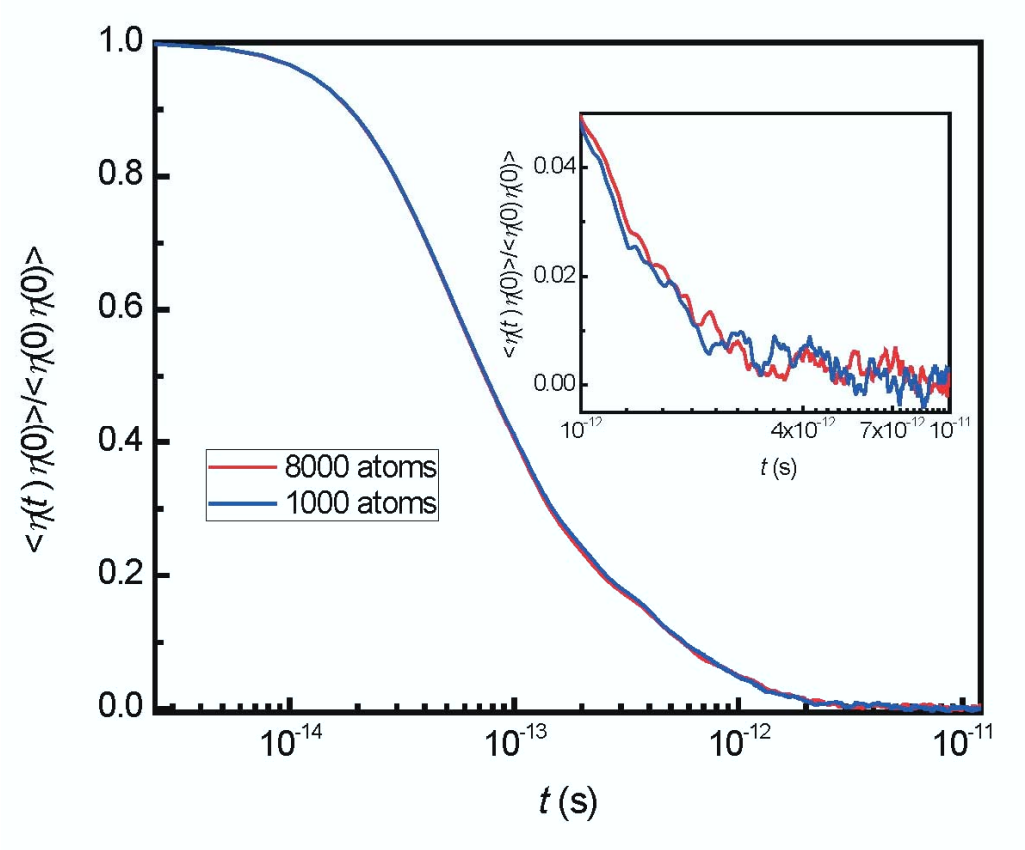

FIG. 12. Normalized stress tensor autocorrelation function at 1800K for samples of 1000 (blue line) and 8000 (red line) atoms.

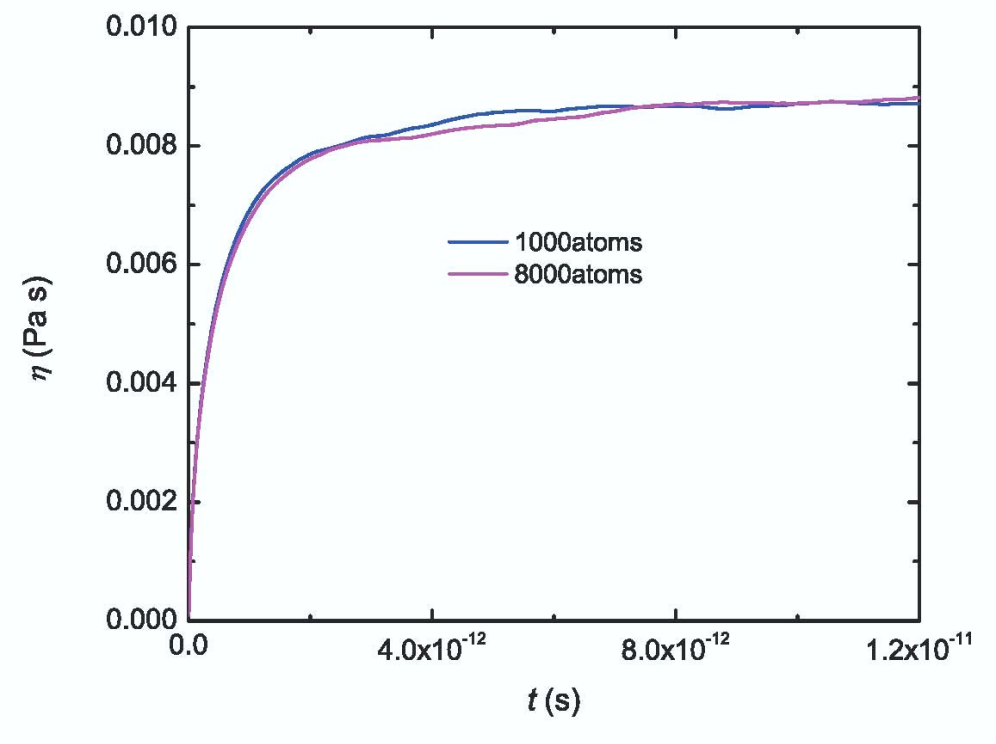

FIG. 13. Viscosity of liquid $Cu_{33.3}Zr_{66.7}$ at 1800K for samples of 1000 (blue line) and 8000 (red line) atoms.

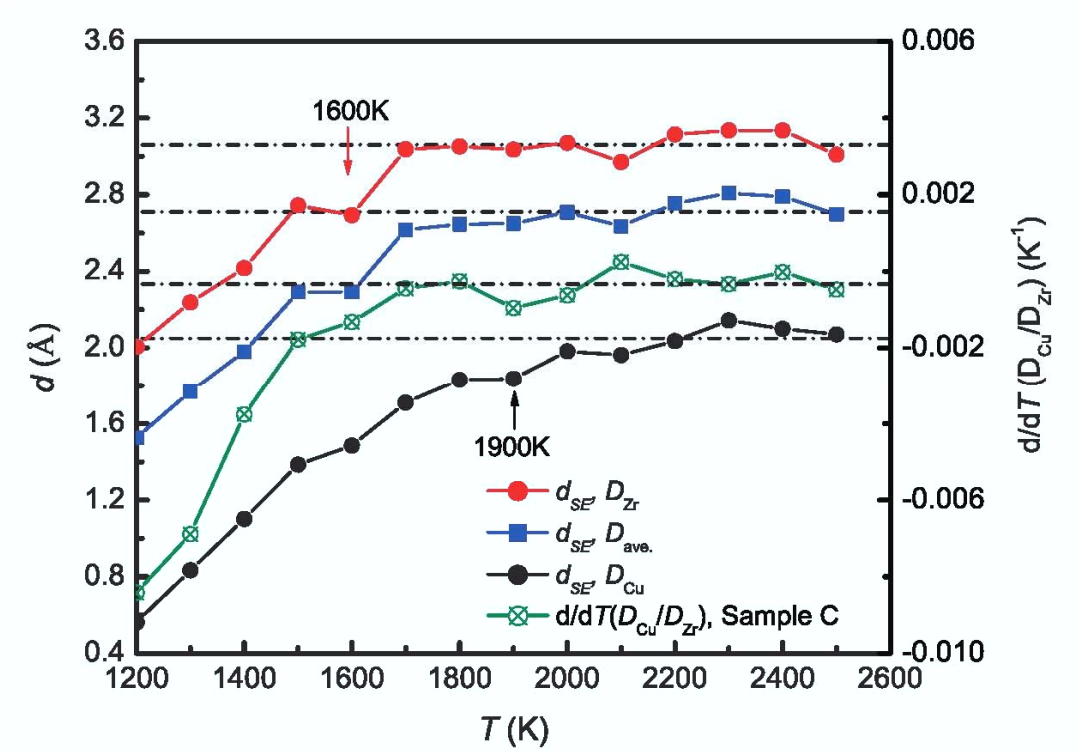

FIG. 14. Effective SE diameters d_{SE}, calculated from D_{Cu}, D_{Zr}, and $D_{aver.}$, and $d(D_{Cu}/D_{Zr})/dT$.

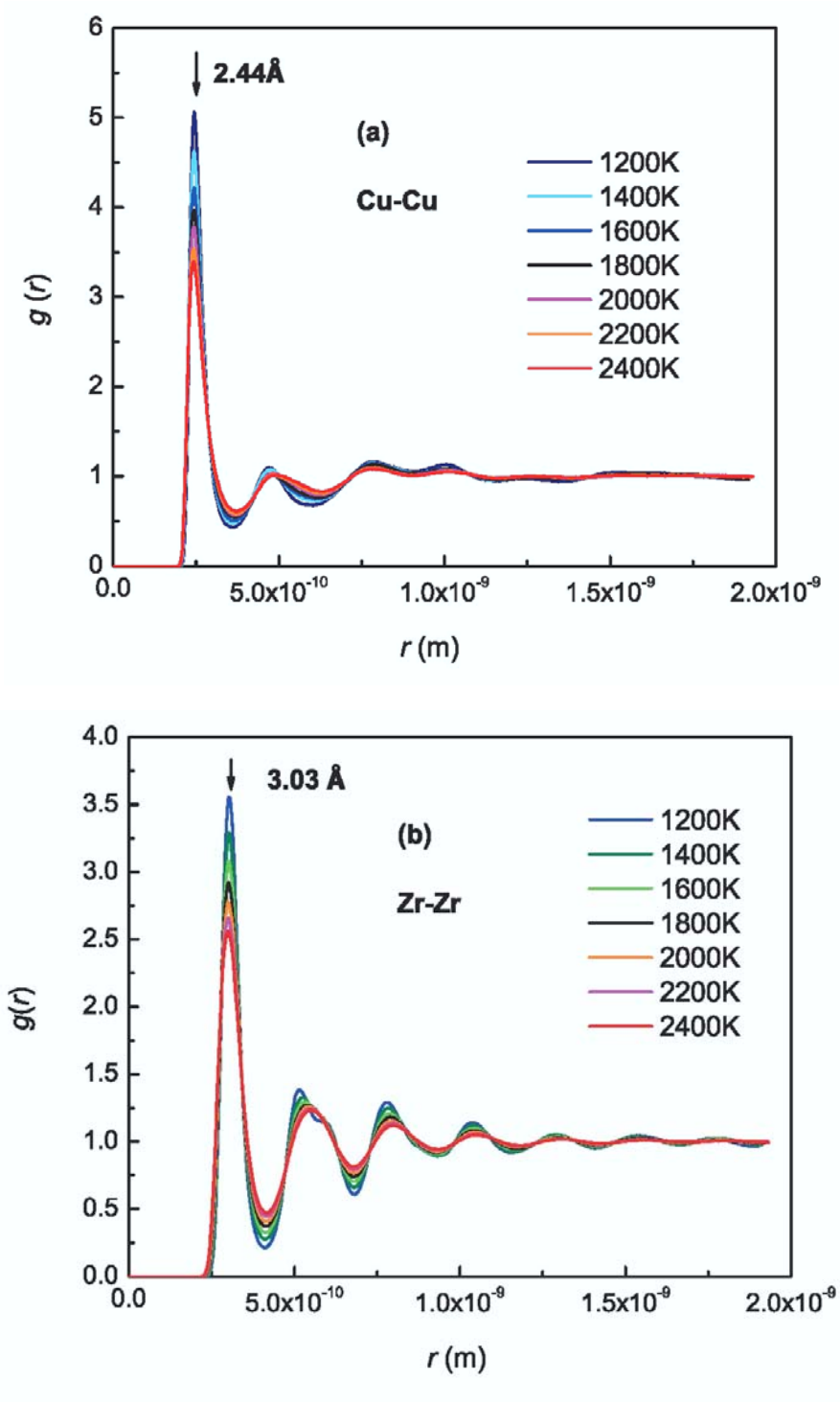

FIG. 15. Pair correlation functions for Cu-Cu and Zr-Zr at different temperatures

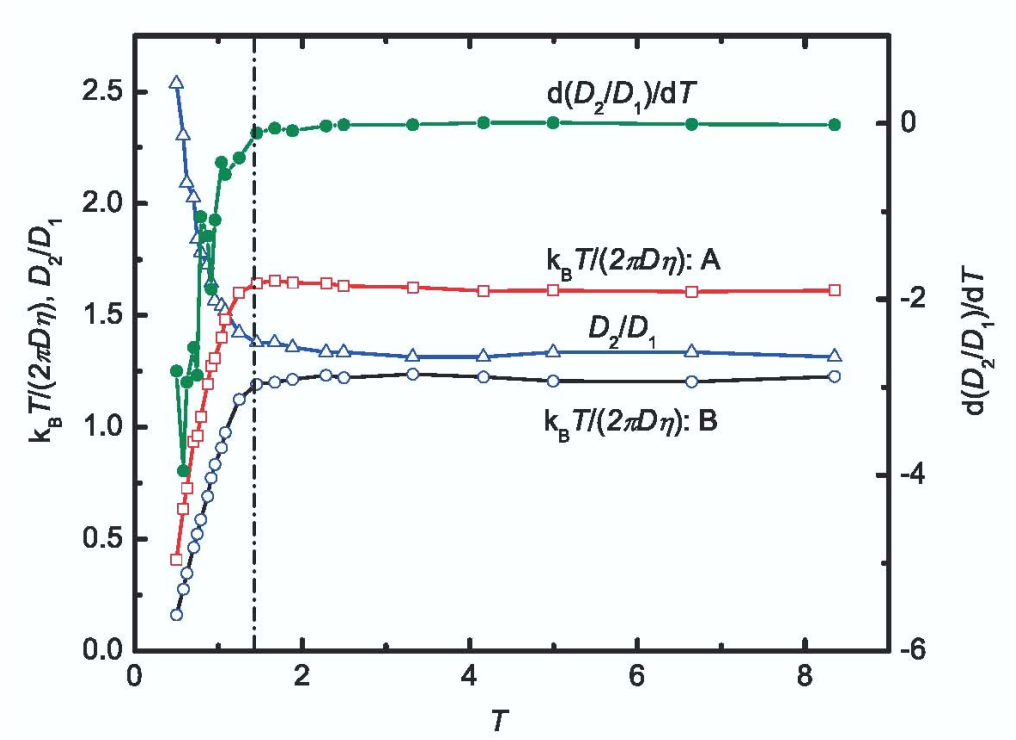

FIG. 16. Effective diameters of the two species, ratio of their self-diffusion coefficients D_2/D_1, and its first derivative for a binary Lennard-Jones system, reproduced from Ref. 17. The effective diameter has the unit of σ_1 , $\mathrm{d}(D_2/D_1)/\mathrm{d}T$ has the unit of k_B/ε_1, where k_B is the Boltzmann's constant, σ_1 and ε_1 are the length and energy parameter for the first component.

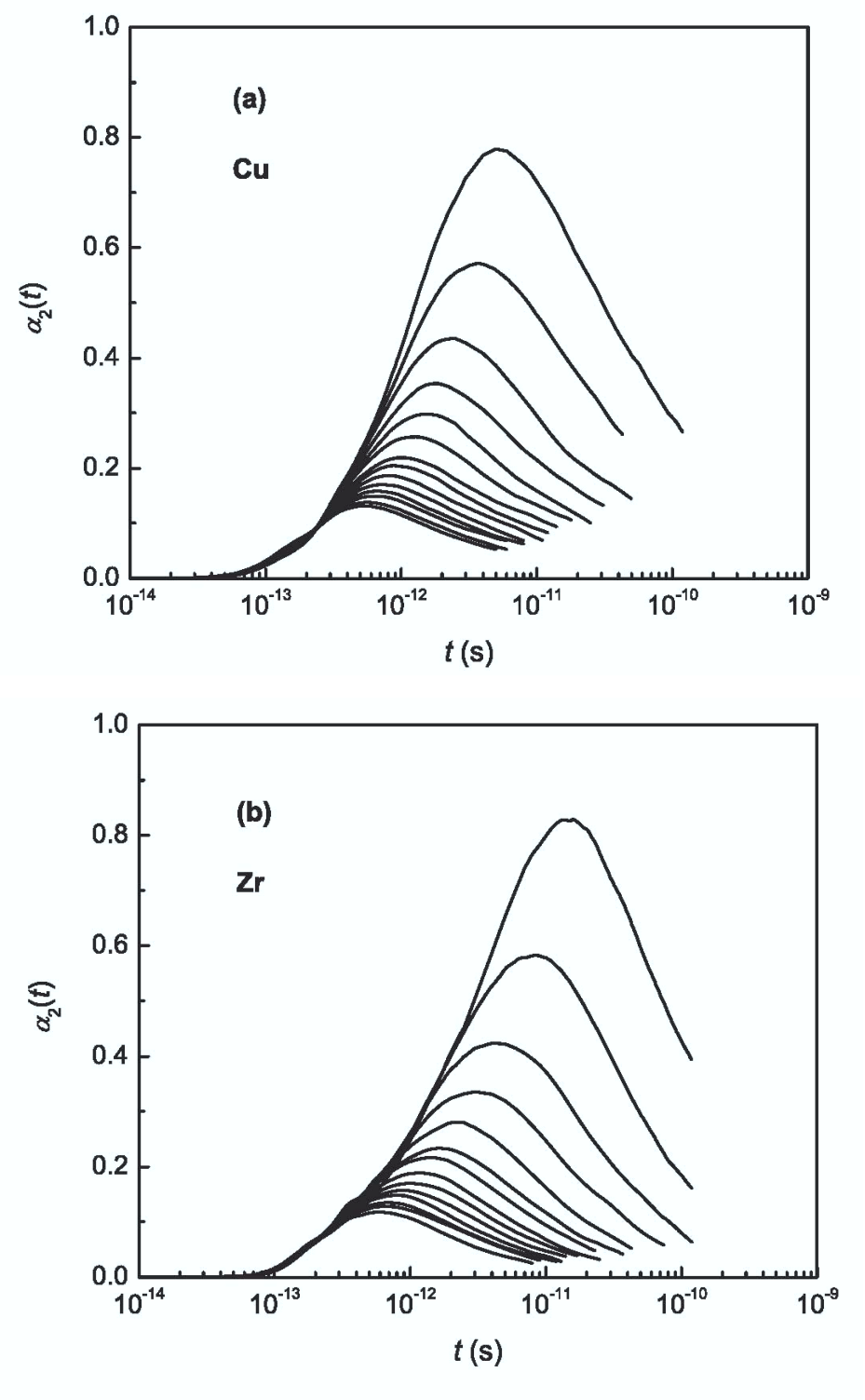

FIG.17. Non-Gaussian parameters for Cu and Zr in liquid $Cu_{33.3}Zr_{66.7}$ at different temperatures (from low to top, the temperature changes from 2500K to 1200K with a step of 100K)

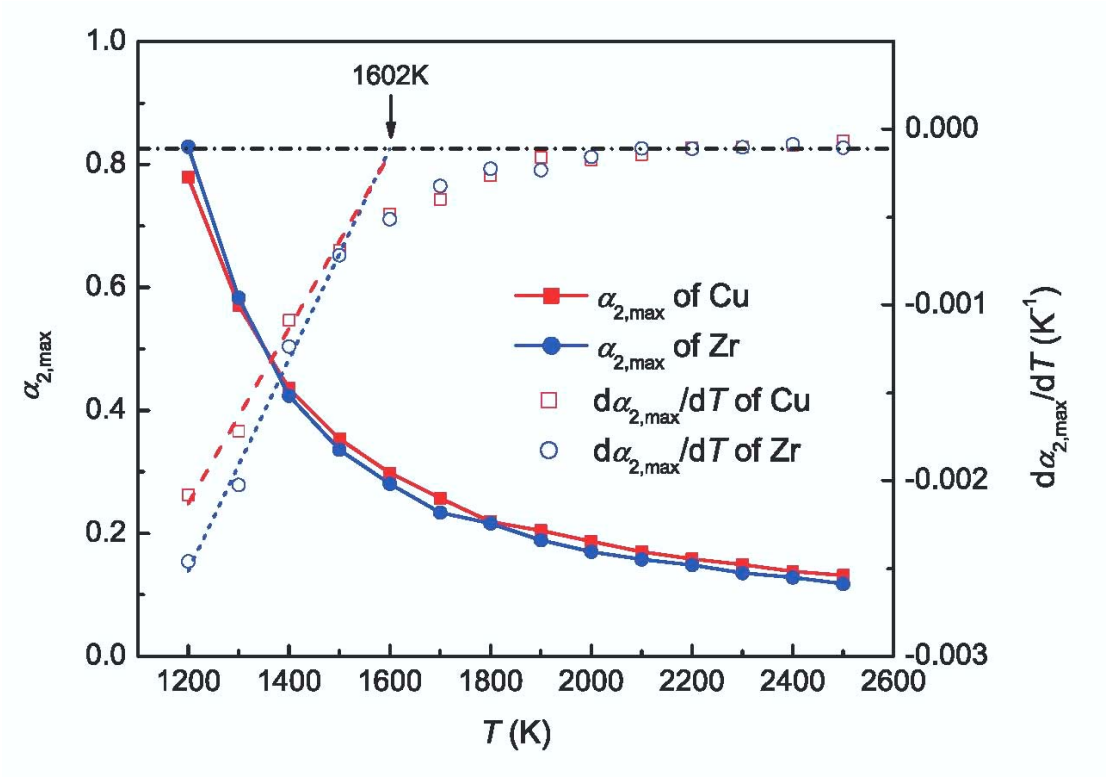

FIG. 18. Maximum of the non-Gaussianity parameter α_2(MAX) and its first derivative for Cu and Zr liquid $Cu_{33.3}Zr_{66.7}$ against temperature

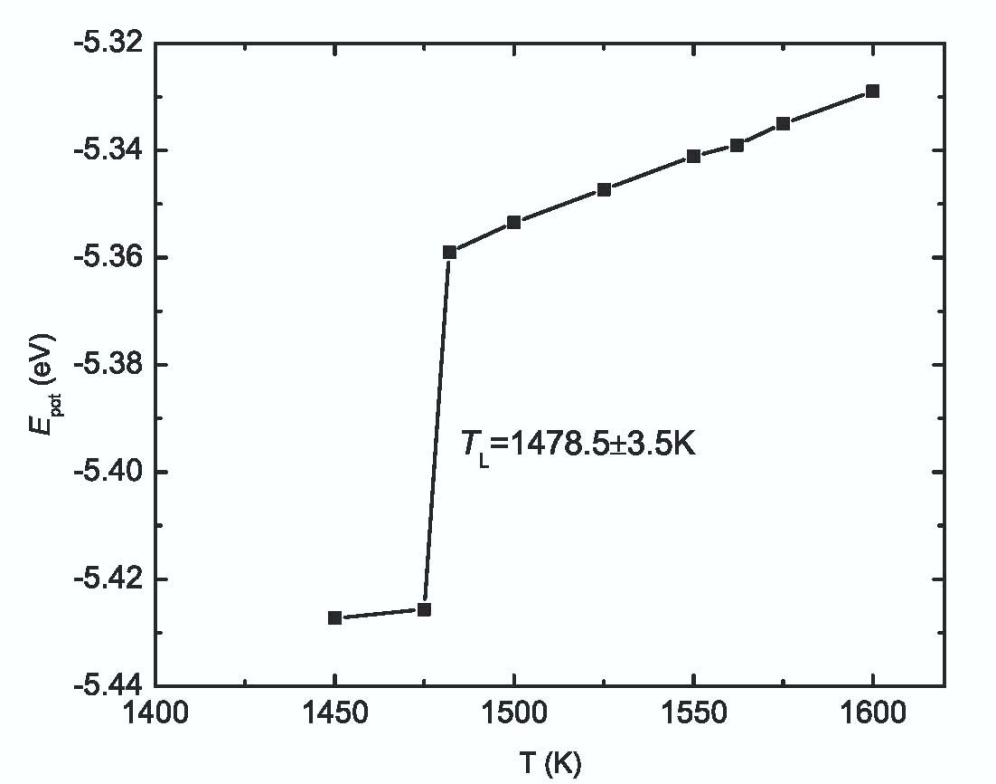

FIG. 19. Potential energy of the coexisting structure at different temperatures.

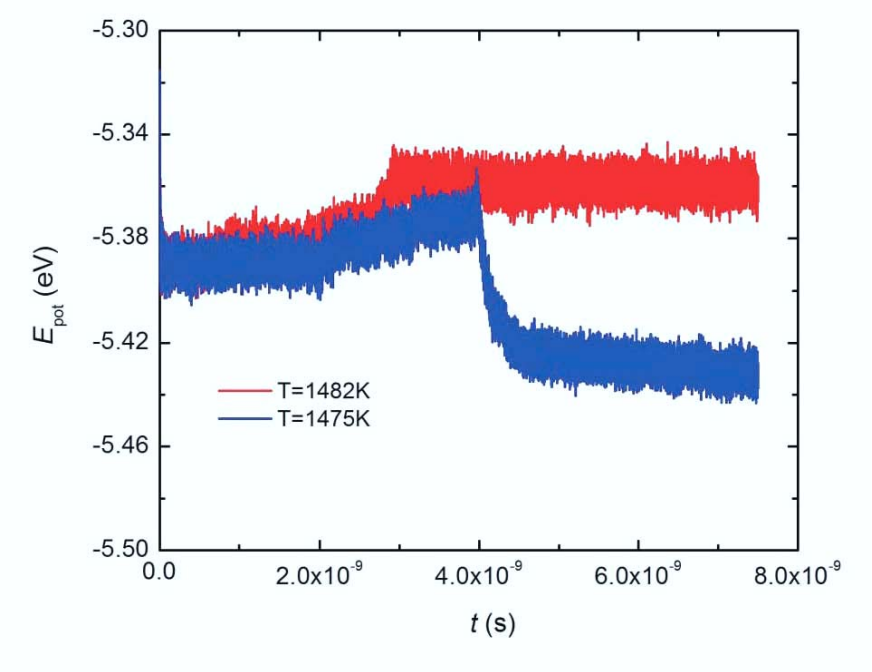

FIG. 20. Variation of potential energy for the coexisting structure during simulation at two different temperatures.